TRANSMISSION-RECEPTION ANTENNA SYSTEM FOR THE EOLE SATELLITE

Translation of "Système d'aériens émission-réception pour satellite EOLE"
Report No. 418, C.F.T.H./C.N.E.S., Massy, 24 February 1965

(NASA-TM-89764) TRANSMISSION-RECEPTION ANTENNA SYSTEM FOR THE EOLE SATELLITE (NASA) 94 p

N88-70764

Unclas
00/32 0140224

NATIONAL AERONAUTICS AND SPACE ADMINISTRATION
WASHINGTON APRIL 1965

CONTENTS

Compagnie Française Thomson-Houston /003*

Electronics Group

I. INTRODUCTION

The purpose of the present report is to describe in detail complementary studies related to the Eole project, in reply to the questions asked by the NASA representatives. This includes:

1) Reppening the satellite project to improve reception without any loss due to the rotation of the plane of polarization (Faraday effect).

2) Narrowing down the technological development conditions, as far as the technical specifications are concerned.

These problems are covered in four different points:

1) Satellite antennas

2) Satellite transmitter (power stage)

3) Satellite receiver (improvement of the threshold by narrow-band filters)

4) Satellite receiver (combiner of polarization diversifier)

Influence of the Faraday Effect:

The studies which have been carried out have shown that the Faraday effect introduced a disturbance which in practice affected only the ballons located near the equator. During the discussions with NASA it seemed that the French project Eole was valuable indeed as a complement to the US project, inasmuch as it permitted tracking balloons located near the equator. It is for this reason that it was decided to modify the project so as to reduce to a mimimum the statistical gain loss due to /004 the Faraday effect.

*Numbers given in the margin indicate the pagination in the original foreign text.

For this the satellite was modified so as to be able to transmit and receive with two mutually orthogonal linear polarisations.

The study of the antenna described below was carried out in order both to solve the radio electronics problems which are present, and to simplify the satellite integration and the launch procedure. This antenna is indeed compatible with a structure stabilized by symmetric gravity; it therefore does not have a spin effect due to the residual gases of the space environment.

In addition, the inversion of the satellite orientation direction is replaced by an electronic phase shifting of a network of antennas, thus permitting orienting the radiation pattern toward the earth.

The satellite transmitter's own power has been increased twofold in order for it to have the same power as in the originial project for each one of the two mutually perpendicular polarizations. A quadrature set-up of the two transmitters, which transform the two linearly polarized transmissions into a circularly polarized one, permits the results obtained from the transmission from the satellite to the balloon to be practically independent of the Faraday effect.

This increase of the peak power is possible without having to redesign the satellite supply system because of the sufficiently great amount of reserve power available in an average consumption condition. This amount of available power is still insufficient to permit replacing the many transistors by a highly reliable electron tube. An increase of the power supplied seems therefore necessary

The balloon equipment have been kept the same (vertical polarization /005 of the antenna) so as to retain both the simplicity of the balloon antenna and the protection against the reflected beam.

The studies related to narrow-band filters have been continued so as to reduce the satellite reception threshold. These studies have confirmed that the proposed solution was not only feasible , but could also work with development components/certain reliability. Filters with similar characteristics (and which in addition are the subjects of original C.F.T.H. patents) have already been installed on the ground equipment. This gives more weight in

support of this type of filter for the solution to the problem involved here.

These narrow-band filter devices have been judiciously complemented by a simple frequency automatic control which permits reducing simultaneously the threshold and the distortion introduced by the filter.

The recovery of the content of the transmission from the balloon to the satellite is obtained by the possibility of electing the plane of polarization in the satellite receiver, because the antenna system gives two receptions in mutually perpendicular planes of polarization.

A study of the various solutions has shown that the simplest was to have the satellite receiver perform a successive exploration of four polarization conbinations spaced 45° apart. During a reception of the signal, a logic verification of the spectral analysis of the signal, which is made by the combination of a multiple resonator filter and the A.G.C. on a complete exploration cycle, stops the switch on the polarization which gives the maximum field.

I - INTRODUCTION /008

The present project proposal is about a satellite radiation system designed to transmit and receive signals at the frequency of 400 MHz ± 50 kHz and to be carried out within the framework of the Eole project.

The desired radio characteristics for the radiating device were the following:

- the highest gain possible for angles ranging between 63° and 73° with respect to the satellite axis
- attenuation of this gain between 5 and 6 dB for an angle of 40° with respect to the satellite axis
- maximum attenuation for all angles less than 40° and greater than 73°
- the device must have two outputs: one output for transmission corresponding

to a circular polarization (right or left), and two receiver outputs corresponding to two orthogonal polarizations (crossed linear or inverted circular).

In addition, certain special conditions had to be taken into account. These are:

- installation on an almost cylindrically shaped satellite having the following approximate dimensions: height: 1 m; diameter: 50 cm /009
- the necessity of taking care of the size problems before installation in the satellite and always taking care of the weight problems
- the desire to free the top and bottom ends of the satellite where stabilizers could be installed.
- the expectation of being able to electrically invert the radiation pattern in order to compensate for a possible inversion of the satllite.

These latter conditions all favor the adoption of a resonating system made up of a network of antennas mounted on the side surface of the satellite. Such a device permits us indeed to completely free the bases of the cylinder-shaped satellite and to permit the radiation to be inverted by means of simple electrical switching.

Such a network presents the added advantage of permitting a large degree of fitting in the elevation and azimuth radiation patterns. This may be done by varying spacing, amplitude and phase parameters in the network source of supply.

II - CHOICE OF THE ELEMENTARY ANTENNA /010

The choice of the elementary antenna was dictated by the size problems encountered in the rocket stage. In spite of the fact that aerodynamic drag imposes no restrictions in space, the use of protruding antennas leads to mechnical deployment problems which are worth eliminating whenever possible. In addition, previous knowledge acquired from applications

concerning air and rockets permits us to extrapolate without any difficulty into the solution offered by antennas which are made flush with the walls for aerodynamical reasons. Finally, there are no serious size limitations inside the satellite which would lead to penalizing the presence of cavities.

It is for these reasons that we have geared ourselves to the adoption of cavity type slit-loaded flush antennas.

The necessity of having two orthogonal polarizations has led us to choose crossed slits. A diagram of this is shown in Fig. 1. These slits are excited by two orthogonal probes (Fig. 1) which feed them into two crossed modes. If these slits were mounted on an infinite reflecting plane the pattern along the plane of each slit would have a lobewidth of approximately 90 degrees 3 dB away and in the perpendicular plane it would be 180 degrees 3 dB away. This is why an intermediate aperture of approximately 130° could be expected in the plane of excitation.

It seemed interesting to us to make preliminary measurements on a reduced scale model in order to experimentally evaluate the action of the cylinder making up the satellite upon the pattern of the proposed antenna.

The dimensions of the cylinder were 25 x 50 cm and the frequency used in the measurement 670 MHz, which led us to a real diameter of about 42 cm.

The results of these measurements are shown in polar coordinates in Figs. 2 and 3. This is the radiation along a cone of 70° angle with respect to the axis (angle of maximum radiation).

It can be seen that the width of the lobe varies between 116° and 150°, depending upon whether the excitation is vertical or horizontal.

These are, of course, only preliminary tests, and the study can yield closer results for the two excitations by optimally adjusting the angle between the two slits and the length of each slit.

III - CALCULATION OF THE NETWORK /012

The proposed network is made up of 3 superposed stages of 3 crossed slits, therefore of a total of 9 elements (Fig. 4). The horizontal network of 3 elements will permit us to obtain an almost omnidirectional azimuth pattern, and the vertical network of 3 stages will be used to obtain the desired elevation directivity.

A. Azimuth Radiation

The azimuth radiation pattern has been calculated graphically starting from the measured patterns of Figs. 2 and 3, and making the following approximations: no coupling between elements and the respective phase centers (identified at the cross section of the two slits).

The results are shown in Fig. 5 and 6. It is seen that the ratio $\frac{\text{maximum}}{\text{minimum}}$ varies between 2.5 dB and 3 dB for the two excitations.

Recall that this is a pattern for a stage having a 3-fold symmetry. If the three stages are successively shifted by an angle of 40° (Fig. 4), a 9-fold symmetry is obtained. In this way a ratio $\frac{\text{maximum}}{\text{minimum}}$ of about 1 dB can reasonably be expected, or a fluctuation of $\pm$ 0.5 dB.

B. Elevation Radiation /013

The choice of the spacing between the elements and the choice of the phase shift between them have been made by trial and error, by a typical network calculation starting from an elementary elevation pattern analogous to that of a dipole.

The spacing chosen in this way was 0.5λ, with a supply constant in amplitude and with a phase shift of 90° between the elements.

The calculation was done by neglecting interactions between the elements.

The results of the calculations are shown in Fig. 7, a comparison with the ideally required diagram. It is seen that deviations in the useful zone are small, in spite of the fact that the attenuation in the other zones is obviously not zero.

It seemed interesting to us to calculate, by graphically inegrating the radiation pattern, the expected directivity of such a device.

Fig. 8 shows curves of $\left(\frac{E}{E_{max}}\right)^2 \sin \theta$ for the calculated network and for the ideal antenna. This is an example of graphical integration calculation.

The results of the calculation give 4.92 dB for the proposed /014 antenna as against 7.30 dB for the ideal pattern.

A more detailed study of these results shows that most of the 2.4 dB deviation between the two patterns is due to the radiation near the horizon of the proposed network (cross-hatched zone, Fig. 8). One does not exclude the possibility of finding a slightly better compromise by having the radiation lobe closer to the satellite axis.

With good quality circuits, a real gain of up to 4 dB with respect to the isotropic case can reasonably be expected.

IV - MORPHOLOGY OF THE SATELLITE /015

The choice of a lateral radiating device with electric inversion entails a few consequences, as far as the geometry of the satellite is concerned. It is essential that the geometry of the satellite have a horizonthal plane of symmetry if the patterns are required to be correctly inverted.

The solution to choose must in addition be compatible with the space available in the carrier rocket. The solution which seemed to us the most rational consists in having two oppositely oriented cones (Fig. 9). On this figure are shown the available space, the shape of the initial satellite and that of the proposed satellite. Note, however, that this solution

leads to a reduction in the surface area of the radiating energy of about 11 %. The total area goes in this way from 1.8 to 1.6 m^2.

V - THE PROPOSED SYSTEM /016

Fig. 10 shows a perspective view of the satellite with all its antennas. It can be seen that a system of 136 MHz antennas was designed. Three rods are installed at 120° spacings in order to maintain the symmetry of the stage of corresponding slits. In addition, these rods have been located on the common base of the two cones in order to retain the geometrical symmetry of the satellite (inversion of the radiation pattern).

We depart of course from the normal cylinder considered in the theoretical calculation of the pattern. It is not excluded that the two cone arrangements of the elements may be favorable from the standpoint of secondary lobes (this arrangement leads to a non uniform radiation of the satellite, with a slight attenuation at the two ends).

Fig. 11 shows schematically the principle involved in combining the elements, the top and bottom connection and the transmission and reception connection.

III - SATELLITE TRANSMITTER /028

III.1 - Background

We have seen that the disturbance introduced by the Faraday effect necessitated the use of two mutually perpendicular linear polarizations.

The radiated power is in this way doubled. The transmission channel can be represented either by a single 40 watt transmitter feeding the two antennas through a 3 dB coupler, with a phase shift of $\pi/2$; or by two

20 watt transmitters feeding two ninety degree signals separately into each antenna.

We have studied a completely transistorized transmitter with a tube in the power stage.

III.2 Transistors Available for the Power Stage

The transistors which were previously thought of for the satellite transmitter were RCA transistors of type TA 2616.

After consulting the US manufacturers of these semi-conductor elements, we have chosen the RCA type 40279, which is a high-reliability version of the type 2 N 3375, and which is designed for space applications. This transistor is of the same family as type TA 2616 but is less powerful.

The number of transistors must therefore be increased. The curves furnished by RCA for the 2 N 3375 specifications show that four transistors are necessary to yield 28 to 30 watts at 200 MHz.

We prefer to retain the use of the varactor-type frequency doubler, /029 which permits us to operate the transistor far from its cut-off frequency and to obtain a good efficiency and a phase shift of the output signal small with respect to the input signal.

III.3 Hybrid Coupling of the Power transistors

The coupling of VHF power transistors by means of hybrids was the topic of a detailed description in the paper entitled: "Hybrid coupled VHF transistor power amplifier" by R.M. Kurzrok, S.Y. Mehlman and A. Newton, I.E.E.E. Transactions on Aerospace, Volume 2, Number 2, April 1964.

This device leads to greater reliability of the individual components and to a lesser number of complete breakdowns; this in turn leads to a greater reliability of the whole system.

A modular construction is possible and facilitates the adjustment procedure.

Note that this particular set-up will become obsolete when a sufficiently powerful transistor will become available.

It would therefore be profitable to take advantage of the time spent on the study for testing the TA 2616 as a space component. It will probably pass the test since this transistor is of the same family as the 40279.

Because of the operating frequency the hybrid is replaced by the lumped constant circuits of the equivalent diagram (Fig. III.3.1).

For a perfect hybrid the power applied at input 1 is divided into two equal parts at terminals 2 and 3, with a power fed atthe terminal 4.

The hybrids are in practice frequency-sensitive devices and they /030 approach the ideal performance only at the calculated center frequency.

The low modulation rate permits only this case to be considered. From the article referred to above the results obtained are in practice:

Power separation 3.35 ± 0.25 dB

Isolation $\geq$ 20 dB

III.3 Description of the Transmitter

The block diagram of the transmitter high level is shown in Fig. III.3.2.

In this figure there is an amplifier stage A_1 located before the first hybrid H_1, the latter being used to feed the two transmission channels.

H_1 feeds a hybrid H_2 and a hybrid H_2'. Between H_1 and H_2' we have installed an adjustable $\lambda/4$ phase shifter designed to give a quadrature between the two output signals of the two channels. The two transmission channels are identical.

The H_2 hybrid feeds two amplifiers A_2 and A_3, identical to A_1.

Between H_2 and A_3 we have a phase equalizer which is a $\frac{\pi}{\lambda}$ radians network equivalent to an adjustable 50 Ω transmission line. The adjustment is made for the maximum output power.

The hybrids H_3 and H_4 feed each two high-power amplifiers A_4, A_5, and A_6 and A_7.

Each amplifier delivers 7.8 W.

The hybrids H_5, H_6 and H_7 provide coupling between the amplifier /031 outputs. At the output of H_7 the available power is 28 watts.

We thus have a varactor doubler which yields an output power of 200 watts at 400 MHz.

The total power consumption by the amplifiers is 159 watts, including the stages which were not described here.

The average consumption of the transmitter is $Pm = 159 \times \frac{12.8}{256} = \frac{1}{2} 8$ watts

III.4 Phase Shift as a Function of the Temperature

Changes in the self inductance and capacitance elements could lead to a phase shift of the signals given by the hybrids and by the amplifiers. Calculations made using a value of 150×10^{-6} per degree centigrade for the temperature coefficient of the elements indicate that the phase changes introduced into every section must not exceed the following:

1° 15' for every hybrid
4° 20' for the amplifier circuits
1° 15' for the phase shifter.

Note that for two parallel sections it is the relative phase shift which is of importance. Since the elements are identical, only the deviations between the temperature coefficients enter into consideration. These can be made very small by selection or by having matched pairs.

The phase shifts introduced by the transistors, and their behavior as a function of temperature are not known, but the preceding remark is

applicable here. In this case it is easier to minimize deviations because these transistors operate far from their cut-off frequency.

III.5 Composition

The transmitter will be made up of a certain number of modules as follows:

1. Hybrid
2. Phase equalizer
3. 4.5 W Power amplifier
4. 7.8 W Power amplifier

The amplifiers have their inputs and outputs matched for 50 Ω and are independently adjusted. They are connected to the 50 Ω hybrids through 50 Ω coaxial cables.

III.6 Use of a Tube for the P.A.

Because of time limits involved in analyzing the problem we have not been able to have systematic information on special tubes for space applications in the 400 MHz frequency band.

We have therefore made a selection from the tubes designed for aircraft inborne equipment which are particularly strong against shocks and vibrations, but we did not have information concerning their lifetime.

Generally speaking the tubes which deliver an amount of power of about 40 watts consume for the cathode heater an amount ranging between 6 and 10 watts.

The pulse repetition frequency does not tolerate a pulsed supply to the filament, which would anyway shorten the life of the tubes because of the repeated thermal stresses applied to their filaments (solution with quick-heating tubes).

VI - Table of Additional Weights and Consumption

VI.1 - Consumption:

		Increase:	
Receiver (1)	: 0.330 W	+ 0.030	+ 0.030
HF input ends and polarization combiner	: 0.050 W	0.050	0.050
Transistorized transmitter	: 8 W	+ 3.600	
Tube type PA transmitter	: 16.25 W		+ 11.850
		3.680 W.	11.930 W.

VI.2 - Weights and Volumes

			Increase:			
	Weight	Volume	Weight	Volume	Weight	Volume
Receiver (1)	: 1050gr.	800cm^3	200gr.	100cm^3	200gr.	100cm^3
HF input ends and polarization combiner	: 140gr.	120cm^3	140gr.	120cm^3	140gr.	120cm^3
Transistorized transmitter	: 1900gr.	1410cm^3	1350gr.	960cm^3		
Tube type PA transmitter (2)	: 1350gr.	1160cm^3			800gr.	710cm^3
			1690gr.	1180cm^3	1140gr.	930cm^3

(1) Not including the H.F. input ends and the antenna polarization combiner which constitute a separate set.

(2) Including the DC-DC converter.

A calculation was made for the tube 3 C P N 100 A 5, which is a radiatorless version of the type 7815 R/ 3 C P X 100 A 5 (plane structure ceramic triode).

The characteristics of this tube lead to the following working conditions:

Heater voltage	:	6 Volts
Heater current	:	0.9 min. 1.05 max Amps
Plate supply potential	:	900 volts
Average plate current	:	0.12 A
HF power delivered by the tube	:	55 W
Output circuit efficiency	:	0.8
Effective HF power	:	44 watts
Average plate dissipation	:	2.65 watts
Power consumption	:	108 watts
Overall efficiency	:	40.6 %
Input power	:	7.6 watts

The input power should be less than 9 watts because of the efficiency of the coupling circuit between the I.P.A. stage and the P.A. tube.

This amount of power can be furnished by a varactor doubler supplied at 200 MHz by 13 watts through two 40.279 transistors coupled by hybrids.

These transistors would be supplied by a power level of 3 W from the low power stages obtained from the initial project.

The block diagram of the transmitter is shown Fig. III.6.1 /034 In addition to the already described stages we have an output coaxial hybrid which provdes distribution of the power to the two antennas.

A phase shifter made up of an adjustable $\lambda/4$ coaxial cable provides a quadrature of the transmitted waves.

The average power consumed by the transmitter is:

Heater power	:	6 W
P.A. Supply power	:	108/20 = 5.4 W
Supply of the transistorized stages:		40/20 = 2 W

The heater voltage (to be determined) and the plate voltage are to be furnished by a dc to dc converter, whose efficiency is 80 %.

$$P_t = \left(11.4/\eta_c\right) + 2 \simeq 16.25 \text{ W}$$

The construction of the transistorized part will be identical with that of the above described transmitter.

Since the tube power amplifier is of the grounded grid type, the cathode and plate circuits will be made up of coaxial cavities.

IV - NARROW BAND FILTER OF THE SATELLITE RECEIVER /038

IV.1 Filter Principles

The proposal considered the sectioning of the whole band, this corresponding to the maximum frequency excursion of 50 KHz, into several channels of 10 KHz band width.

In November 1964 the filter optimization was still unfinished but the studies were continued so as to be able to determine the feasibility of the proposed device.

These studies were made with the following assumptions:

1) The total 50 KHz band was sectioned into elementary bands by 80 single pole resonators. A limited number of resonators (from 5 to 6) of consecutive rank and selected from these 80 are put in parallel so as to constitute a filter of 40 KHz band width. A decision logic chooses the center frequency of this filter within the total bandwidth, depending on the levels detected by each resonator.

2) The format of the balloon response signal has been slightly modified in order to reduce the systematic distortions introduced into the measurement of distance by the balloon identification character, and also in order to simplify the distributer which provides the signal format aboard the balloon.

The diagram showing the principle involved in the band selector is shown in Fig. IV.1.I.

A detector having a very low time constant is associated with each resonator R and with a threshold device S, which in turn indicates whether or not the detected voltage exceeds a predetermined threshold. This threshold is the same for all the resonators.

A matrix of diodes permits us to open the gates P of ranks /039 n - k to n + km whenever the threshold of rank n is excited. The resonators, whose gates are open, are put in parallel and the output signal of the resulting filter commands the gain of the receiver by means of a usual A.G.C. device.

With the signal present, the receiver gain diminishes and the A.G.C. regulation valve is such that only a number n of threshold detectors are excited.

The threshold value is selected so that n + 2k is equal to the number of resonators which are desired for determining the narrow band filter.

The selection is performed at two different times with the same basic principle, in order to reduce the number of poles and the weight of the equipment. A separation of the functions permits us to simplify the construction (Fig. IV.1.2).

Two analyses occur successively in the two following different filters:

1) The acquisition filter takes simultaneous care of the balloon frequency acquisition, of the frequency advance positioning of the modulation filter, and of the selection of the polarization, following the technique described in Chapter V.

2) The demodulation filter provides narrow band filtering with reduced distortion, which is necessary for decoding the balloon signal and for obtaining precision in the measurement of the distance.

The acquisition filter is made up of 20 poles of bandwidth 1250 Hz at 3 dB, separated by 2500 Hz. The command matrix is such that k = 0. The detection threshold is selected such that one, or at most two, filters are excited when the frequency modulated signal is received with an index of 1 and a signal frequency of 625 Hz (synchronization signals).

The threshold is adjusted for - 4 dB with respect to the reception /040 level, which corresponds to the carrier only at the center of each filter.

The overall bandwidth which makes acquisition possible is 50 KHz (Fig IV.1.3).

The demodulation filter is made up of 7 poles of 1250 Hz bandwidth at 3dB, spaced 625 Hz apart and phase shifted by $\pi/4$. The structure utilized is explained in the following sections. The control matrix is designed for n = 3 or 4 (threshold at - 2.5 dB), and k = 1. Because of the low number of resonators, the structure appears as simple as in Fig. IV.1.4.

This filter completes the acquisition and, in normal operation, the demodulation filter is made up of the five central resonators which together constitute a filter of about 4 KHz bandwidth.

The complete device is shown in Fig. IV.1.2. The last frequency change at the acquisition channel input is at a fixed frequency. That of the demodulation channels, however, has a variable frequency which is determined by an indirect frequency standard simultaneously controlled by the acquisition filter (through the acquisition and diversification logic component), and by an automatic frequency control, tapped after discrimination, from the acquisition channel.

The frequency standard has 39 positions separated in frequency by 1250 Hz. Its discrete values are controlled by the acquisition filter output voltage in such a way that if the frequency of the signal to be received is centered on one of the acquisition filter resonators it is at the same time centered on the middle resonator of the demodulation filter. The even frequency positions (2p x 1250 Hz) are controlled by the only excited resonator. The odd frequency positions [(2 p + 1) 1250 Hz] are controlled on the middle frequency of the two successive resonators which are simultaneously excited.

The use of automatic frequency control permits us to reduce the /041 transit time distortion, while at the same time providing a narrow band filter. The A.F.C. frequency cut-off is about 10 Hz. It is sufficient to provide for centering the frequency which is received by the narrow-band filter at the instant when the fine measurement of the distance is performed, namely during the second half of the signal.

The group velocity distortion introduced during the reception of the identification signal remains high but still acceptable for the demodulator used.

The format of the response signal is modified as follows:

synchronization	52	bits
identification	10	bits
measurement of the temperature	129	bits
measurement of the pressure	65	bits
	256	bits

This format brings to 204.8 ms the duration of the balloon response by increasing the time of the synchronization period (see chapter V).

This format simplifies the balloon distributor. The counting, which is performed in this distributor, is stopped at the beginning of the identification word. The precise determination of the end of the distance measurement signal is performed by the counting done aboard the satellite.

In addition the end of the signal, upon which the fine integration of the distance measurement is done, is made up practically of a 625 Hz sinusoidal signal, to within two phase reversals (corresponding to the temperature and pressure measurements). This reduces the random distortions introduced by the filters into the pseudo random signal.

Feasibility studies were carried out both theoretically and experimentally. Calculations were made:

1) On linear phase shift resonator filters already studied by C.F.T.H. for analogous studies;

2) In order to determine the distortion introduced into the zeros of the signal which is chopped by the zero shift of a carrier frequency, this frequency being modulated by a sinusoidal signal of 1250Hz.

For the experimental studies we take into consideration the following:

1) Prior studies by C.F.T.H.

2) A study which reproduces on a simplified model of a filter the conditions involved in tests simulated by calculations. The study permits us to have an idea of the order of magnitude of the practical deterioration of the theoretical results.

IV-2- Theoretical Calculations /047

The signal received aboard the satellite has an effective bandwidth of about 3.75 kHz when the first three lines of the 625 Hz frequency modulated signal are considered (modulation index = 1).

Except during the transmission time of the identification signal, the signal is made up practically of an almost sinusoidal signal of 625 Hz frequency.

Because of the Doppler effect and of the oscillator drift, the pass band is widened to 50 kHz. The proposed filter is made up of resonating circuits connected in parallel, 5 or 6 of which are selected or actuated when the carrier occupies the frequency center of the elementary band which is determined in this way.

The characteristics of the narrow band filter are the following:

- center frequency 220 kHz
- number of active poles 5 or 6
- 3 dB bandwidth of a single pole 625 Hz
- steps between resonance frequencies 625 Hz
- phase shift at the input of one pole with respect to the next $\pi/4$

IV-2-1 Filter Calculation (response curves)

The effect of the various parameters is shown by the following various filters which are calculated for a 1250 Hz frequency modulated signal.

1) Zero Phase Shift Filter

A group of 9 poles of zero phase shift at the input of one with respect to the next lead to very unfavorable curves of phase and amplitude, for the proposed application.

The bandwidth of a single pole is chosen to be 1.25 kHz.

The curves of Fig. IV.2.1 show the amplitude and the phase as a function of the frequency. /048

2) Filter with $-\frac{\pi}{2}$ Phase Shifts

A group of 9 poles phase shifted by $-\frac{\pi}{2}$ at the input of one with

respect to the next lead to phase and amplitude curves which are improved over those of the preceding case.

The bandwidth of a single pole is chosen to be 1.25 kHz. The curves IV.2.2 and IV.2.3 for the filter under consideration show both the amplitude and phase vs frequency, and the propagation time as a function of the frequency.

3) Filter with $-\frac{\pi}{4}$ Phase Shifts.

A group of 9 poles successively phase-shifted by $-\frac{\pi}{4}$ lead to phase, amplitude, and time propagation (in the filter) curves which are still better than those obtained above for the proposed application. The curves IV.2.4 and IV.2.5 of the filter under consideration show both the amplitude and phase as a function of the frequency and the propagation time as a function of the frequency. The bandwidth of a single pole is chosen to be 2.5 kHz.

4) Optimization of the Frequency Steps.

As indicated above, the F.M. frequency used by these filters is 1.25 kHz. The steps between resonance frequencies have also been chosen to be 1.25 kHz. The advantage presented by such a choice lies in the fact that the carrier and its lines (in the filter) lead to approximately equal changes of the phase shift of the carrier and of its side band frequencies.

Refer to Fig. IV.2.6, which shows phase shifts as a function of the frequency. /049

When the carrier frequency goes from position 1 to position 2, the side bands go from 1a and b to 2a and b. The resulting phase change is about the same, which permits us to limit the resulting distortions.

IV.2.2 Calculation of the Distortion.

We have worked out a calculation program for the distortion introduced into a frequency modulated wave by the above described filters. This program permits us to have the zero displacement of the demodulated wave at the discriminator output, with respect to the zero positions of the modulated

wave without the filter, as a function of the position of the carrier frequency.

We shall go into the results of calculations of the distortion introduced by the filters which are phase shifted by $-\frac{\pi}{4}$ and $-\frac{\pi}{2}$. But before we do this, it is necessary to make the following remark, which applies to both types of the above described filters.

Since the frequency steps of the successive poles are 1.25 kHz, the reduction of the results of distortion calculations must be made by taking the position of the carrier frequency between 220 - 0.625 kHz and 220 + 0.625 kHz. Indeed, when the carrier frequency goes outside the above limits, i.e., when the carrier frequency becomes 220 + 0.800 kHz, the center frequency of the new 9-pole elementary filter becomes 221.25 kHz, after the end poles of the old elementary filter of 220 kHz center frequency have been turned off and on again.

1) Elementary filter made up of 9 poles phase shifted by $-\frac{\pi}{2}$ /050

The curve of Fig. IV.2.7 shows the zero shifts of the modulated wave which are introduced by the elementary filter under consideration with a center frequency of f_o= 220 kHz.

The maximum average distortion calculated when the carrier frequency goes from 220 kHz to 220,625 kHz is of about 1 μ second.

2) Elementary filter made up of 9 poles phase shifted by $-\frac{\pi}{4}$

The curve of Fig. IV.2.8 shows the zero shifts of the modulated wave introduced by the elementary filter under consideration of center frequency f_o= 220 kHz.

The maximum average distortion calculated when the carrier frequency goes from 220 kHz to 220,625 kHz is of about 0.2 μ second.

IV.2.3 Characteristics of the Passband Filter Having a Linear Phase Shift and made by C.F.T.H.

A filter has been made by C.F.T.H. (Bagneux group) for the purpose of solving the problems posed by pulse compression.

The filter is made up of 16 resonating circuits having the same passband. These circuits are uniformly shifted in frequency with cross points at 3 dB, and are fed by signals successively phase shifted by $\frac{\pi}{2}$.

The center frequency of the filter is f_o = 225 kHz and the total bandwidth is 40 kHz.

Result of Technological Tests /051

The changes in the self-inductance of a resonator are from - 0.3 % to 0.2 %, when the temperature ranges respectively from - 15°C to + 60°C.

The changes in the capacitance of a resonator under the same climate conditions are respectively from - 0.1 % to 0.1%.

The frequency drift in the range of temperatures from - 16 to + 60°C is less than 0.5 %.

The transmission time in the passband of the 16 element filter is shown in Fig IV.2.9. Photographs of the filter (black and white slides) are enclosed.

The amplitude response curve of the filter is obtained from IV.2.10.

IV.3 Experimental Verification

We have applied the above described principle. The filter diagram /052 is shown in Fig. IV.3.1. The steps between elementary circuit are 1000 Hertz. The passband of each circuit is 1000 Hz at - 3dB. In order to simplify the adjustment, the phase shifts 0 and $-H$ are made with a transistor. A passive network provides a phase shift of $-\frac{H}{2}$ at the 2nd transistor input

($-\frac{H}{2}$ and $-\frac{3H}{2}$). Gain adjustment has been provided to compensate for insertion losses due to the $-\frac{H}{2}$ network. Note that for the final version, lossless phase shifting networks would be used, with two lattice network sections with $m = \infty$ and $m = 16$.

Note from Fig. IV.3.2 that there is a discrepancy between the theoretical and experimental amplitude vs frequency curves. This drawback is due to the variations between the Q's of the elementary network sections ($\Delta Q \approx \pm 7\%$).

Measurements were made of the group lag as a function of the center frequency of the modulated wave on the rising and trailing edges of the demodulated wave.

We have made a bench model of a stable oscillator with linear and noiseless modulation characteristics (no hum).

With a Tecktronix oscilloscope triggered by the 1000 Hz modulating signal, we measured the group lag introduced by the six-pole filter at the output of a Gertsch demodulator (modified for the experiment). The precise measurement of the center frequency of the modulated oscillator was made with a Hewlett Packard counter.

Since the filter has only 6 sections we have selected a modulation index of 1, with a modulation frequency of 1000 Hz.

Two series of measurements were made: the first one without a filter at the output of the demodulator, the second one with a bandpass filter centered at 1000 Hz inserted between the demodulator and the oscilloscope.

The insertion of a bandpass filter provides elimination of the harmonics and spurious frequencies (hum at 50 Hz, HF residual frequency) and improves the measurement precision.

The results obtained are shown in Fig. IV.3.3. In this figure we have drawn curves obtained by calculation for the phase shifting of the rising and trailing edges. The average phase shift is also plotted.

Note the good agreement between the theoretical curves and experimental results for the right-hand part of the curve and a disagreement for the left-hand part (here the sign is different). We did not have enough time to establish a correlation between these facts and the disagreement observed in the amplitude curve (Fig. IV.3.2), nor to debug the filter.

It is important to note that the absolute values of the calculated and measured errors introduced are of the same order of magnitude:

$$|\text{maximum measured error}| = 2\ |\text{calculated error}|$$

This rapid experimental verification was performed within a few days and the discrepancies observed are most likely due to imperfections in the device.

/054

IV.4 Narrow Band Filtering According to the Diagram of Fig. IV.1.2

IV.4.1 Determination of the Threshold Associated with Each Resonator

The acquisition and demodulation filters include a certain number of threshold detectors which permit a possible removal of the resonators from cut-off.

We have been led to evaluate, for the frequency modulated wave, the level in dB of the peak voltage which is detected at the resonator output, for different positions of the carrier frequency which lies within the frequency bandwidth of the resonator. This was done in order to determine the threshold of the acquisition and demodulation filters.

1) Acquisition Filter. Choice of the Threshold.

The acquisition filter is, as said before, made up of 20 resonators with 1250 Hz bandwidth at 3 dB.

Fig. IV.4.1.a shows the peak voltage level in dB at the output of detectors corresponding to 3 adjacent resonators, as a function of the carrier frequency.

If the threshold level is chosen to be 4 dB it can be seen that, depending on the frequency position of the signal, 1 or 2 resonators are removed from cut-off.

2) Demodulation Filter. Choice of the Threshold.

The demodulation filter is made up of 7 resonators of 1250 Hz bandwidth each at 3 dB, separated by 625 Hz, with the phase shift from one resonator to the next being $\frac{\pi}{4}$.

Fig. IV.4.1.b shows the detected peak voltage level in dB corresponding to several adjacent resonators as a function of the carrier frequency.

If the threshold level is chosen to be 2.5 dB, it can be seen that, /055 depending on the value of the carrier frequency, the number of excited threshold detectors is 3 or 4.

By referring to Fig. IV.1.4, it can be seen for example that if the resonators R4, R5, R6 are excited, the resonator R3 is connected directly to the output, R7 is removed from cut-off by the detector corresponding to the resonator R6, and the resonator R6 is removed from cut-off by the resonator corresponding to the resonator R5.

A total of 5 resonators are put in parallel in this way.

If for example the detectors R4, R5, R6 and R7 are excited, the resonator R3 being directly connected to the output, the number of resonators put in parallel is 5.

If for example the detectors R3, R4, R5 and R6 are excited, the resonators R7 and R2 are removed from cut-off by the detectors corresponding to the resonators R6 and R3, respectively, and the total number of resonators put in parallel is 6.

IV.4.2. The Demodulation Filter Considered /056

The domodulation filter under consideration is made up of 7 poles of 1250 Hz bandwidth at 3 dB. These are sapced 635 Hz apart and the relative phase shift from one pole to the next is $\frac{\pi}{4}$.

In the preceding section we have seen that the number of poles put in parallel is 5 or 6 (see Fig. IV.1.4), depending on the number of resonators excited (3 or 4 depending on the position of the carrier).

1) 5-pole Filter

Fig. IV.4.2.1 shows curves for amplitude and phase shift of a filter made up of 5 poles successively phase-shifted by $-\frac{\pi}{4}$ and spaced by 625 Hz.

The single pole bandwidth is chosen to be 1250 Hz.

Fig. IV.4.2.2 shows the zero shifts of the frequency modulated wave which is introduced by the elementary filter under consideration of f_o = 220 kHz center frequency.

2) 6-pole Filter

Fig. IV.4.2.3 shows curves of amplitude and phase of a filter made up of 6 poles phase-shifted by $-\frac{\pi}{4}$ one with respect to another, and spaced 625 Hz apart.

The bandwidth of a single pole is chosen to be 1250 Hz.

Fig. IV.4.2.4 shows the zero shifts of the frequency modulated wave, introduced by the filter under consideration, of f_o = 220 KHz center frequency.

Analysis of the distortion curves IV.4.2.2 and IV.4.2.4 shows that a distorition of 1 microsecond (average displacement) corresponds to a shift of the carrier of

1) $\pm$ 300 Hz for the filter made up of 5 poles /057

2) $\pm$ 950 Hz for the filter made up of 6 poles

IV.5 Conclusion

The theoretical curves of Section IV.4.2 show that the most unfavorable case of a distortion of 1 μ sec corresponds to that of a 5-pole filter.

By taking a safety factor of 2 the error made on the distance measurement and introduced by the filter can be made less than 1 μ sec provided the carrier center shift is less than $\pm$ 150 Hz.

We can therefore conclude that the proposed device will be able to satisfy this condition if the A.F.C. feedback loop gain is greater than $\frac{1125}{150}$ = 7.5 or 17.6 dB.

This device adds a gain of 4 dB to the threshold, as compared with the use of a filter of 10 kHz bandwidth.

V - DIVERSIFICATION OF POLARIZATION /077

Since the balloon transmission is vertically polarized, the wave received by the satellite is a plane wave whose plane of polarization may have turned by a certain angle because of the Faraday effect.

This angle of rotation depends on a sufficiently large number of parameters (solar activity, distance from the satellite to the balloon, angle between the balloon direction and the local magnetic field, satellite latitude) so that this angle can be considered random.

The theoretical solution, which would permit cancellation of the propagation loss due to the angle between the incident wave and the plane of polarization of the antenna, would consist of using a polarization combiner. This solution would be very expensive since it would lead to having two receivers, including the narrow band filters. The existence of these filters permits us to solve the problem by a much more elegant method, which consists in obtaining cyclically, from two onboard satellite receiving antennas, with their successive planes of polarization making an angle of 45° between themselves.

The polarization switching is performed in a periodic cycle of 4.8 millisec. The time constant of the receiver dead time is less than 2 millisec. That of the receiver is of about 50 to 100 millisec. The time constants of the detection of narrow ban filter resonators are less than one millisecond. Under these conditions the logical use of the command signals of the acquisition filter matrix permits us to make a decision as to the nature of the polarization direction along which the field is strongest. The automatic gain control stores in a memory the strongest field whenever a signal from the balloon is received. Consequently, during the two or three tests following two passes through the plane of polarization which gives the strongest field, no resonator is excited. It is only necessary to stop the /078 sweep when, during the first period following the no-excitation condition of the resonators, the position is that which corresponds to the maximum field, which in turn is characterized for excitation of one or two resonators.

Since the signal which comes from the balloon is capable of arriving at any time within the exploration cycle of all the various polarizations, it is necessary to have at least eight periods of exploration before the arrival of the identification signal. The individual cycle presents in the most unfavorable case a minimum of 4 bits, to take care of the prephasing necessary for the demodulation of the identification signal.

The exploration device necessitates the presence of the electronic switches and of two adders between the antennas and the receiver input.

In order to simplify the embodiment of this device, without at the same time increasing the losses, each of the two sets of antennas with crossed polarizations is connected to a low-loss transmission - reception switch which has a receiving end output connected to a low-noise amplifier. The polarization combination is done on the low-noise amplifier outputs, according to the four following combinations:

$$V_1 , V_1 - V_2 , V_2 , V_1 + V_2$$

The gain loss due to the residual angle between the planes of polarization is always less than 0.7 dB and has an average statistical value of about 0.2 dB.

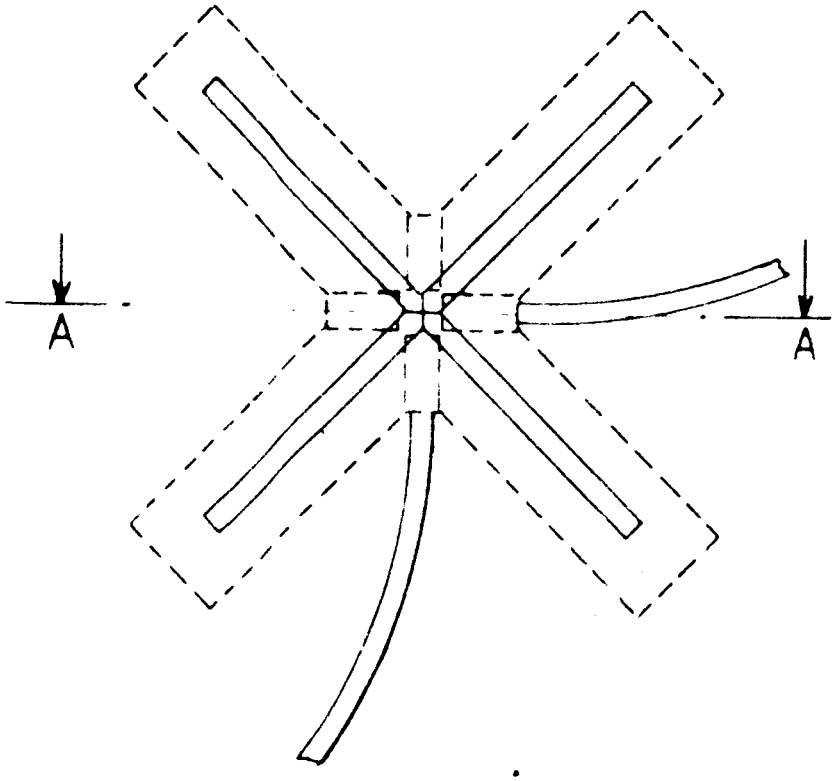

Section AA

Coupe AA

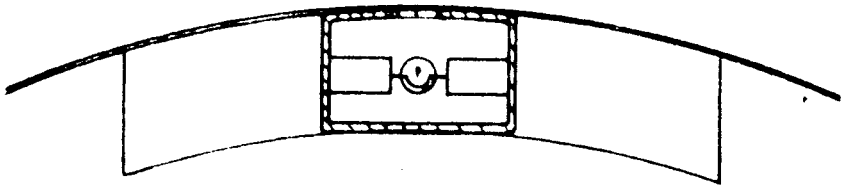

FIG. 1

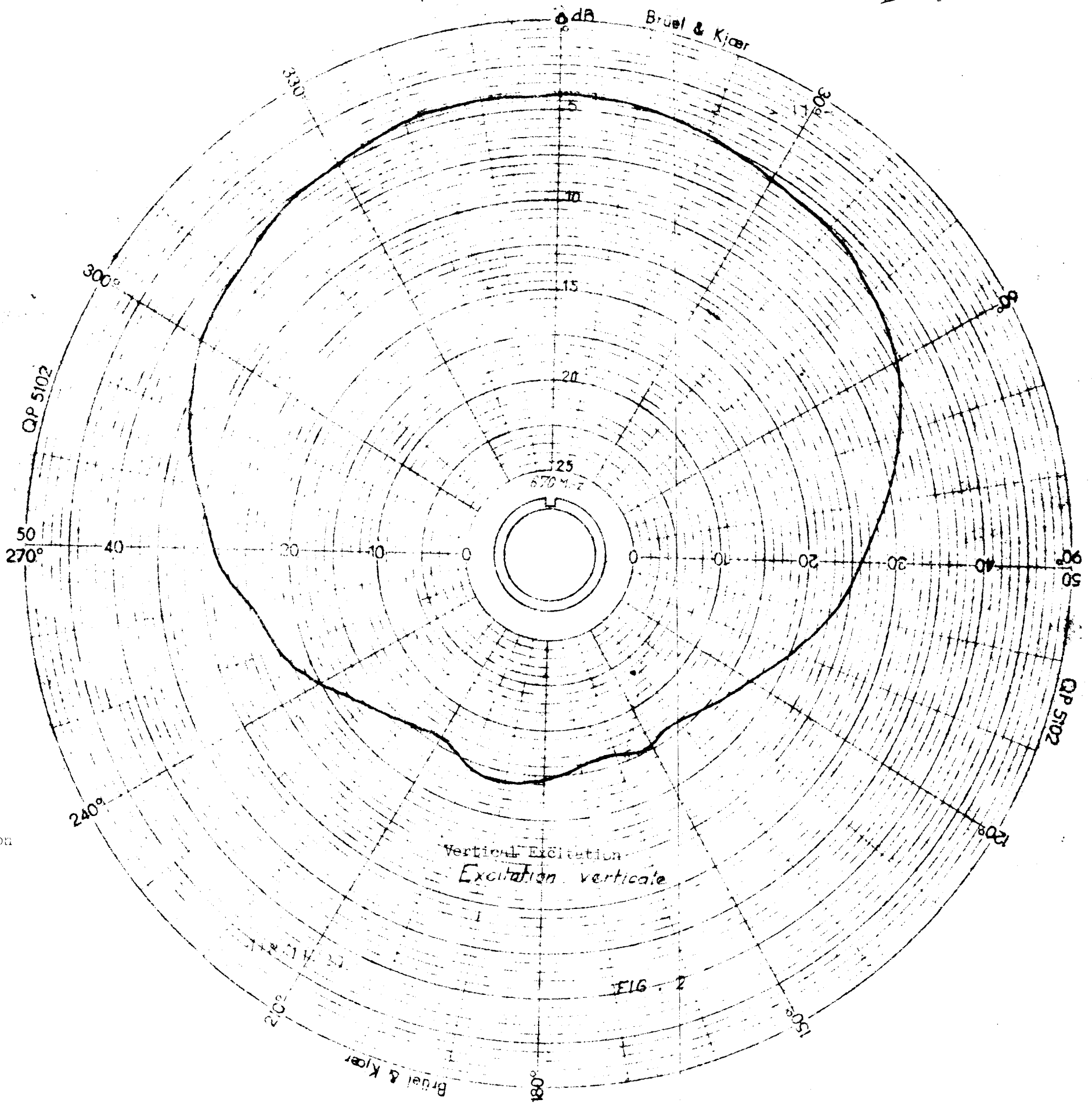

Vertical Excitation

FIG. 2

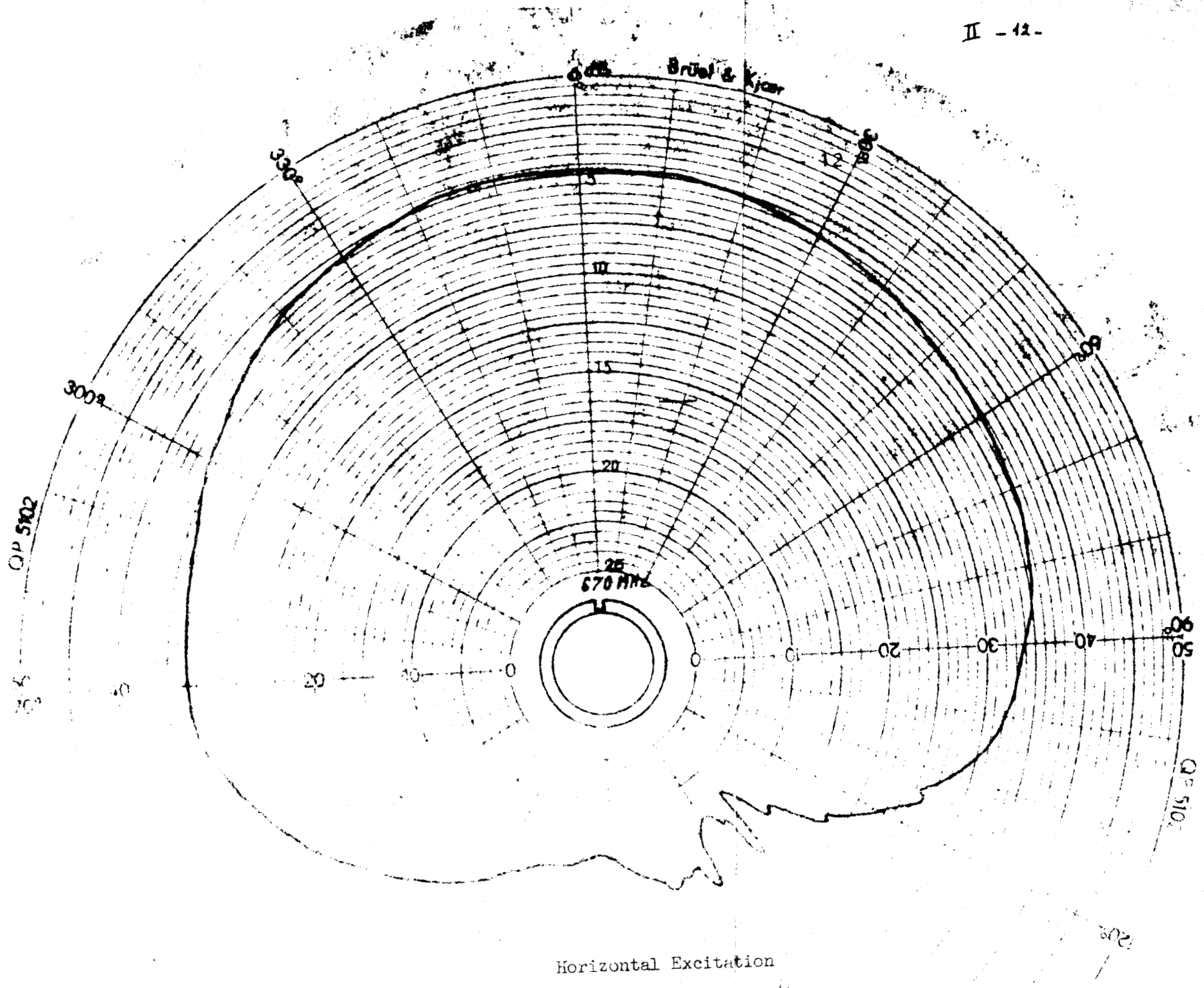

Horizontal Excitation

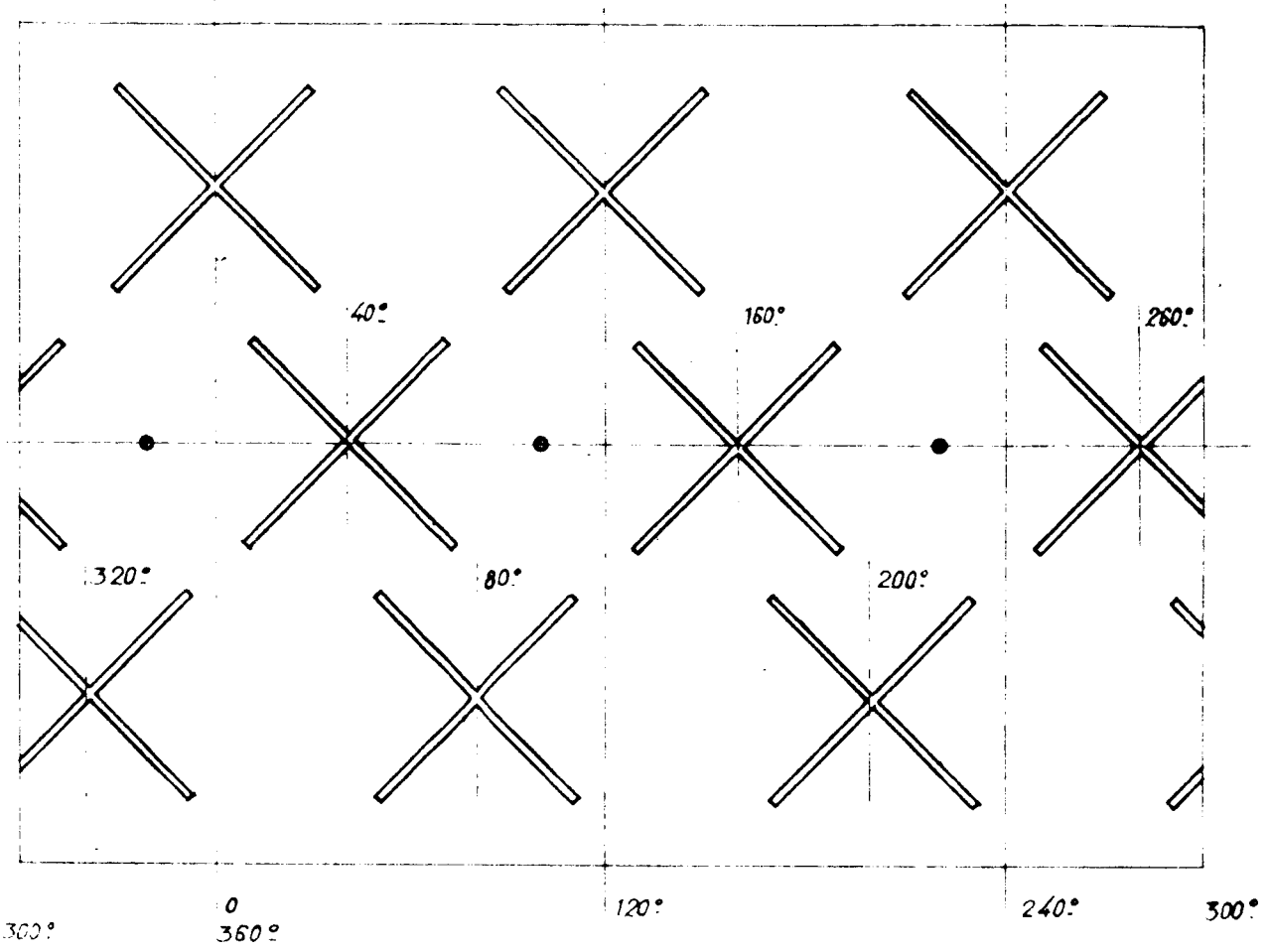

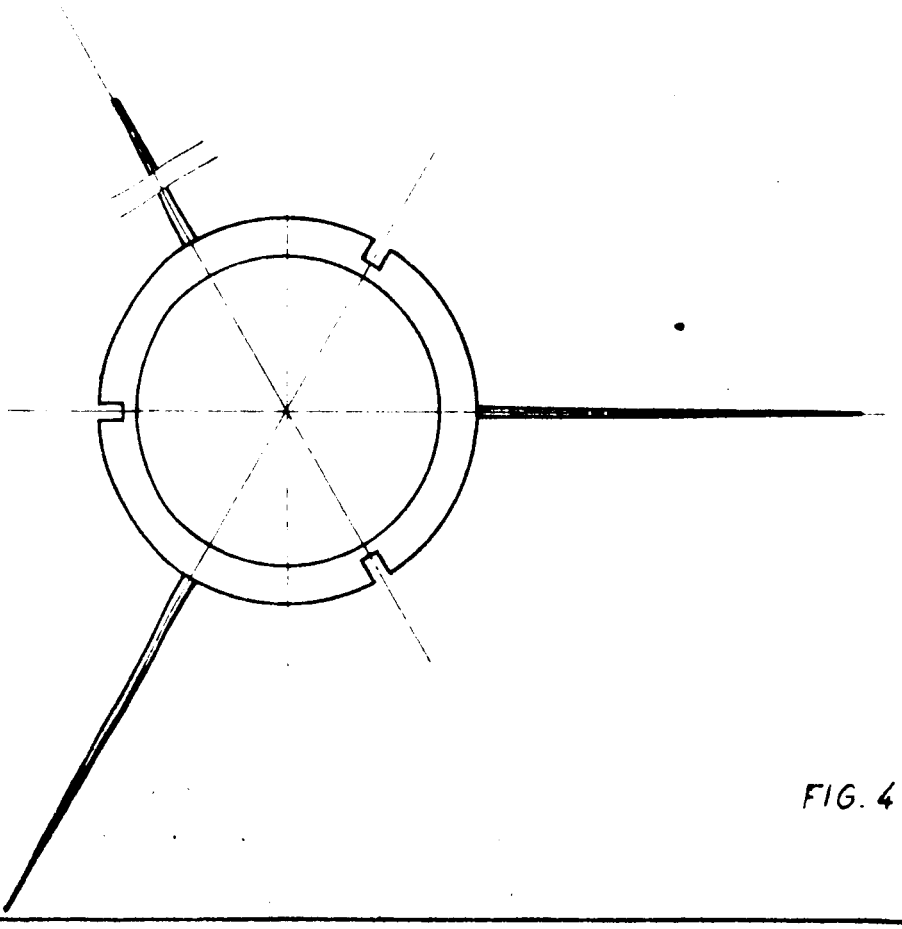

FIG. 4

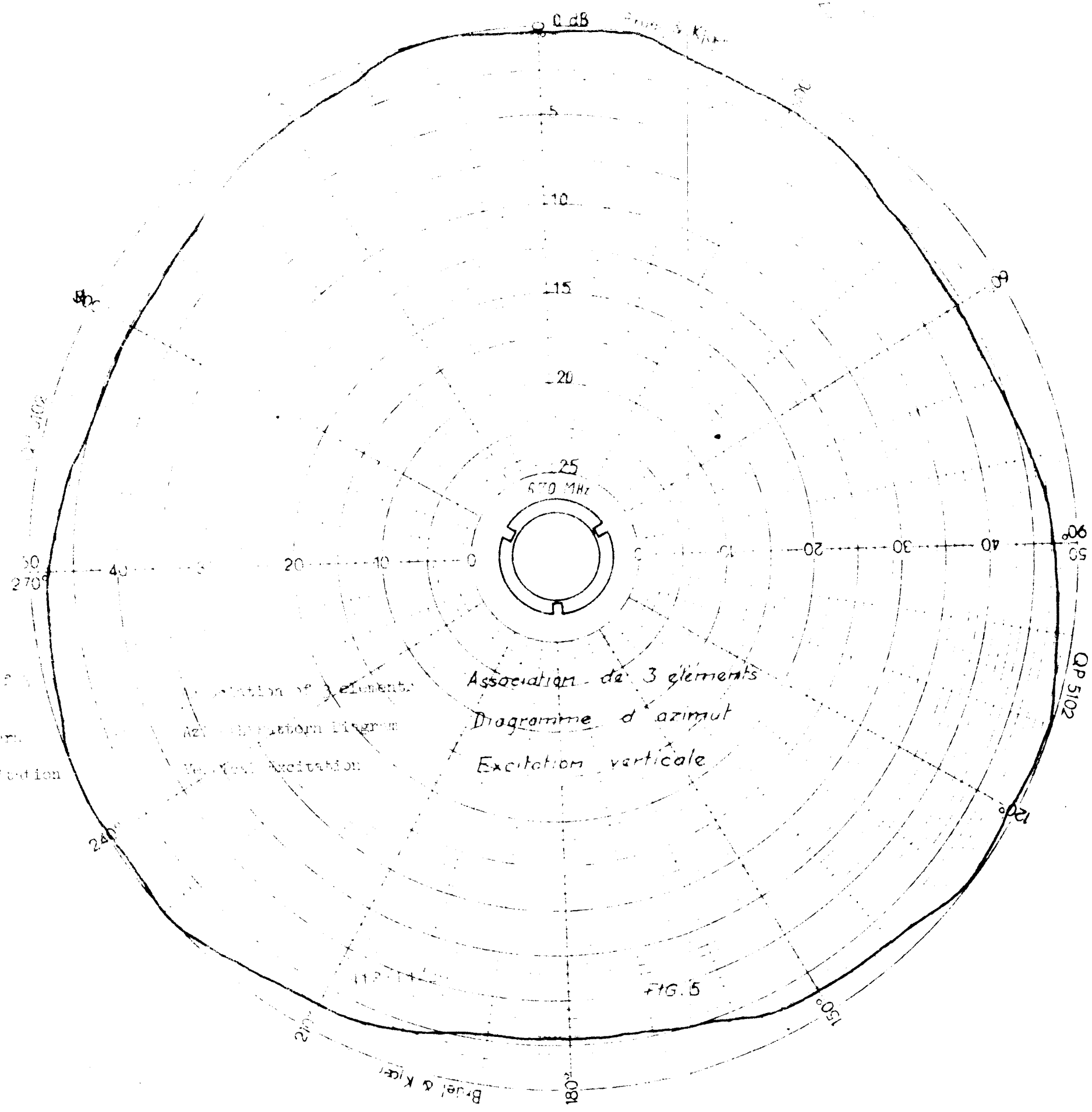

Association de 3 éléments

Diagramme d'azimut

Excitation verticale

FIG. 5

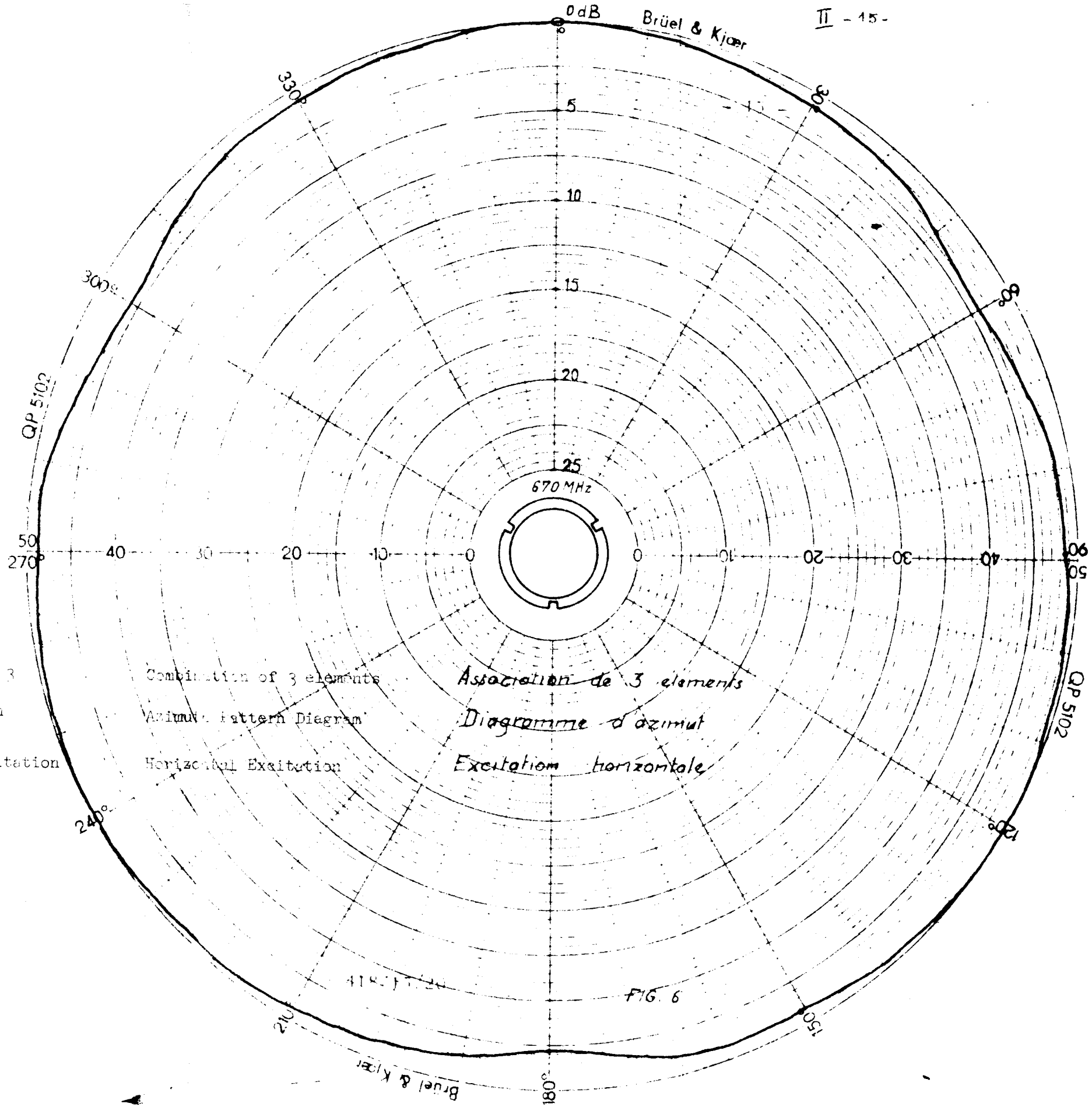

Combination of 3 elements
Azimuth Pattern Diagram

Horizontal Excitation

Combination of 3 elements

Azimuth Pattern Diagram

Horizontal Exaitation

Association de 3 elements

Diagramme d'azimut

Excitation horizontale

FIG. 6

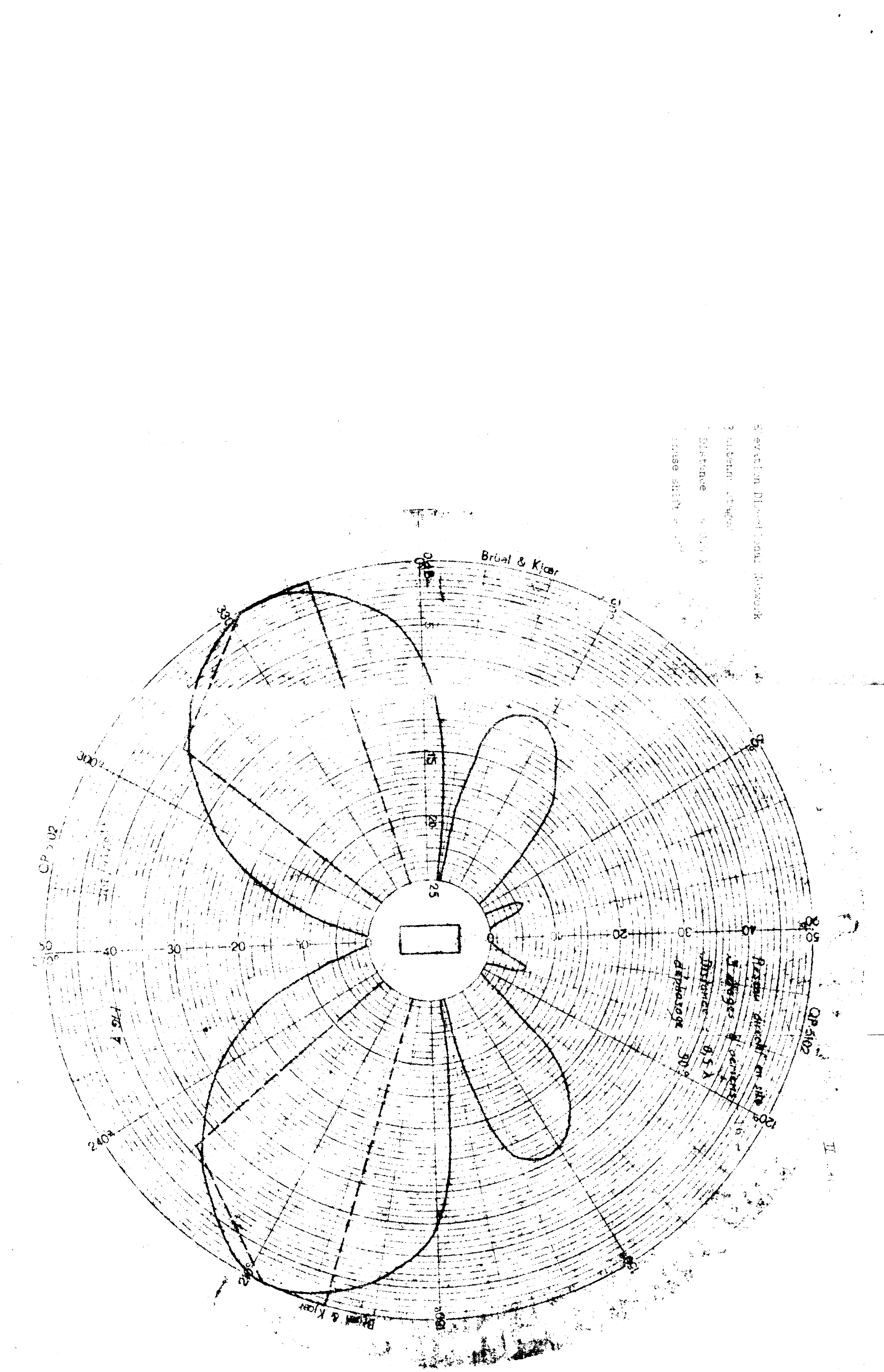
Brüel & Kjær
Type 4144
Microphone Position Dynamic Linear Network
Free field response
Random incidence response
Diffuse field response
Polar diagram
Distance 0.5 m
Type 4144
Brüel & Kjær

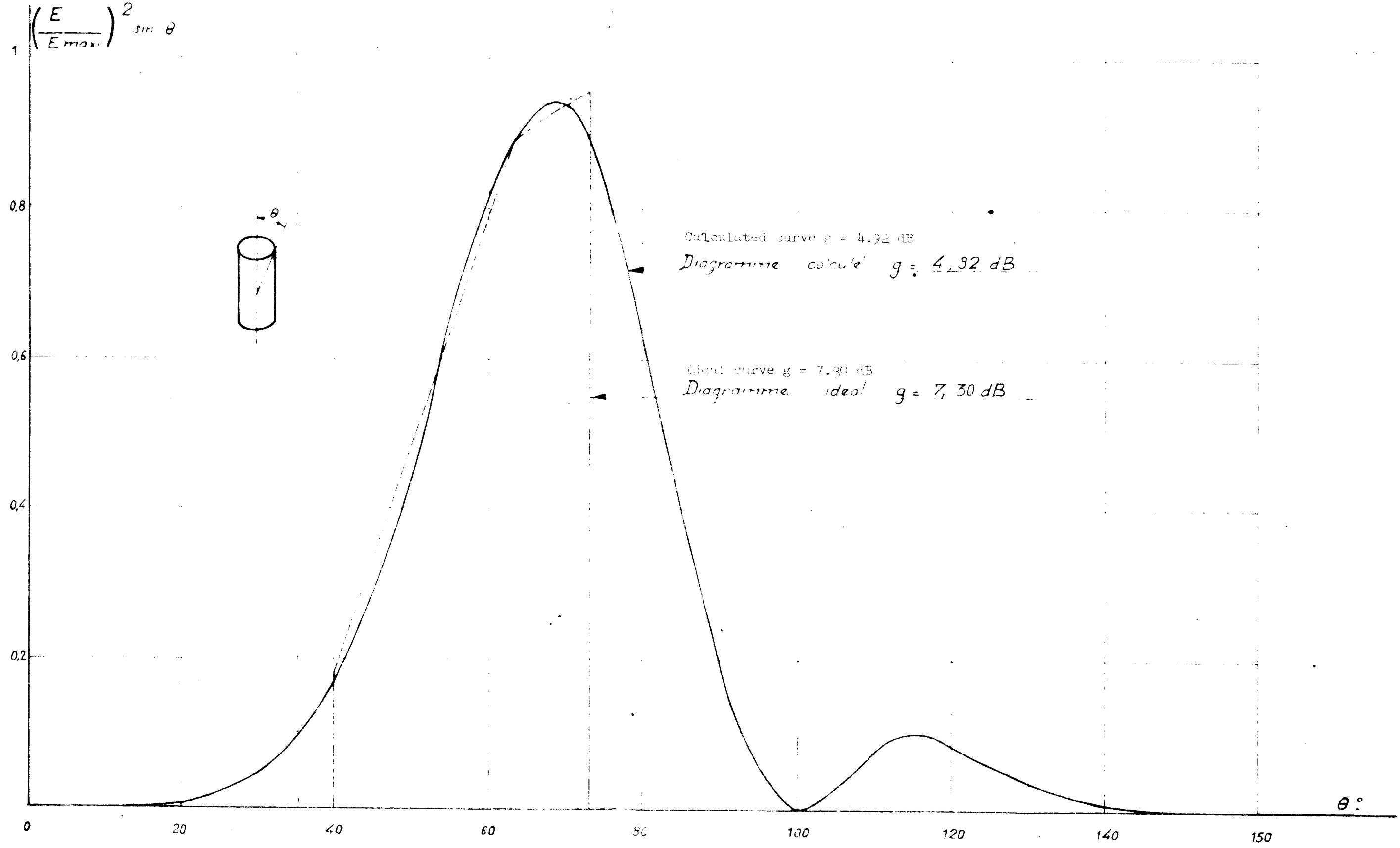

Calculated curve g = 4.92 dB

Diagramme calculé g = 4,92 dB

Ideal curve g = 7.30 dB

Diagramme idéal g = 7, 30 dB

418/17/20

FIG. 8

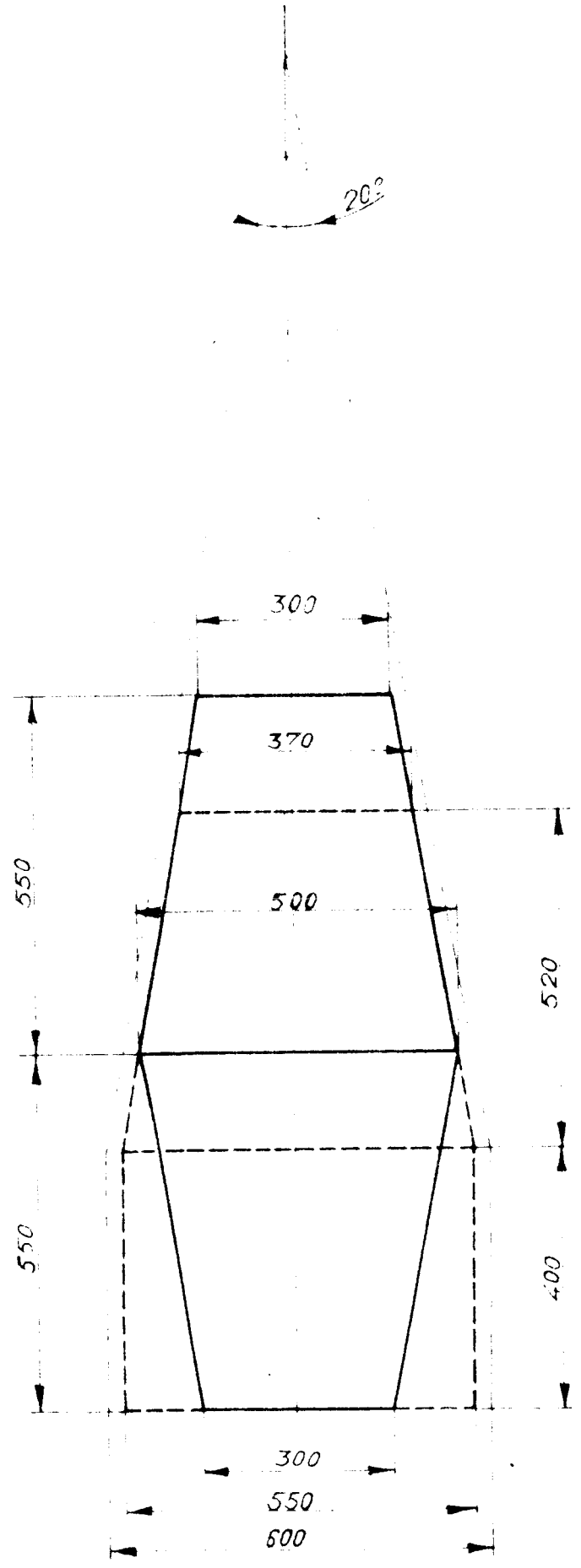

FIG. 9

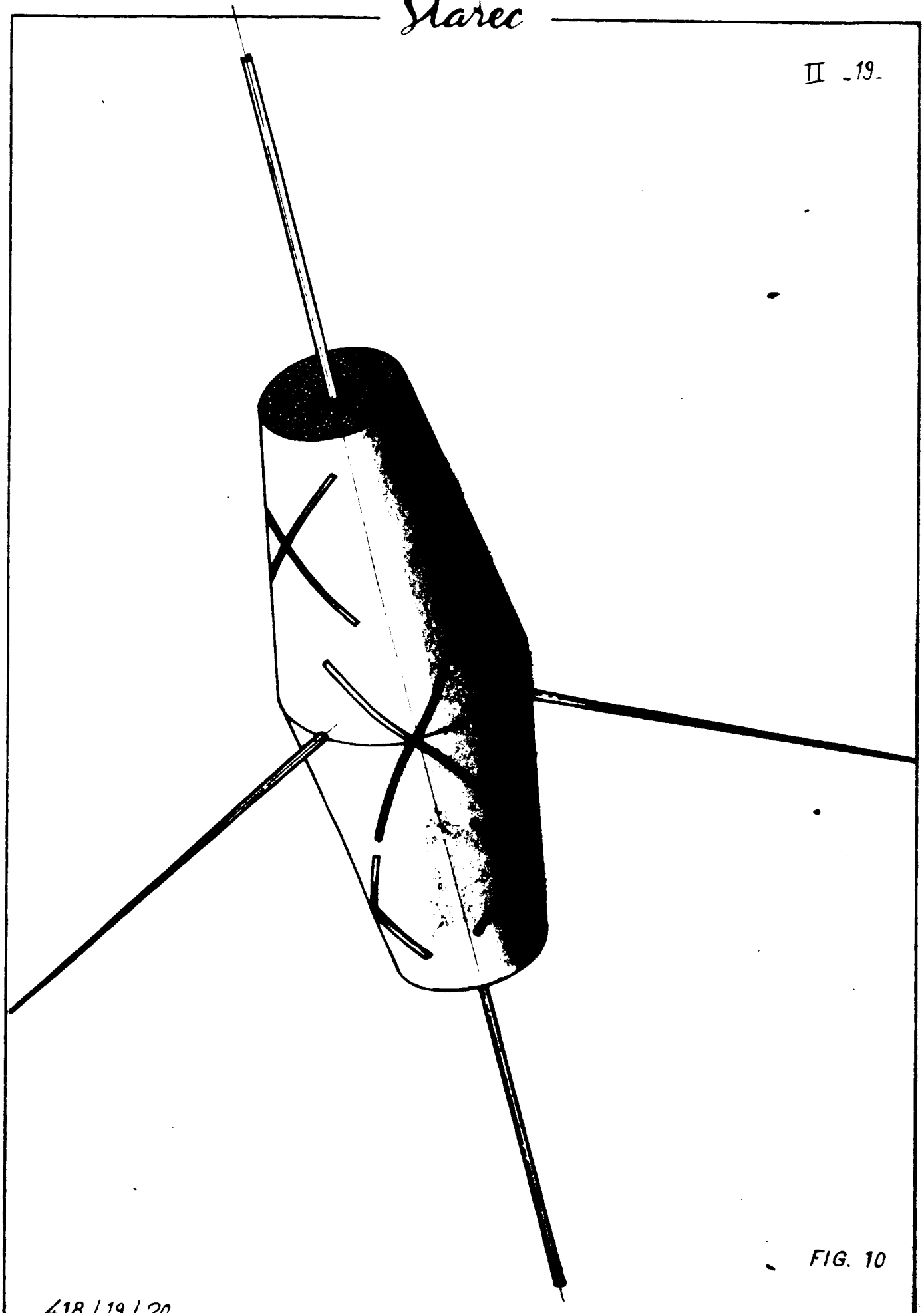

FIG. 10

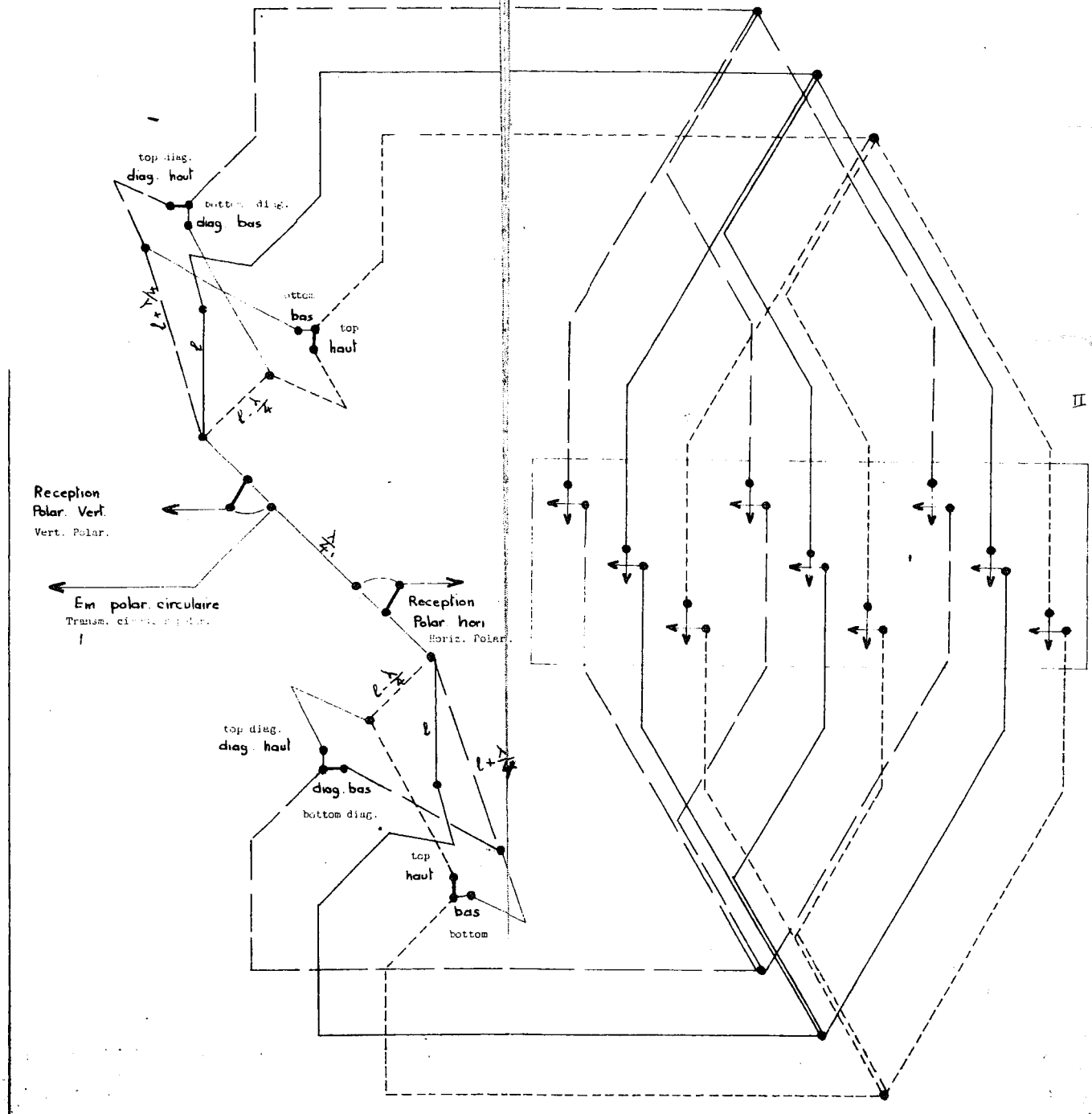
top diag.
diag. haut
bottom diag.
diag bas
bottom
bas
top
haut
Reception
Polar. Vert.
Vert. Polar.
Em polar. circulaire
Reception
Polar hori
Horiz. Polar.
top diag.
diag haut
diag. bas
bottom diag.
top
haut
bas
bottom

Fig. 11

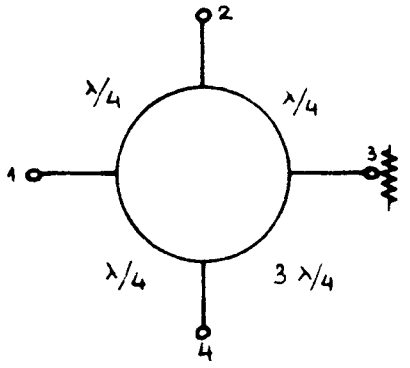

Diagram of the hybrid
Représentation de l'hybride

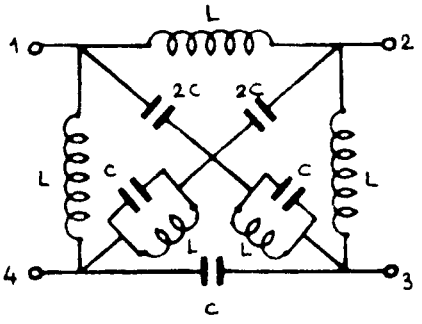

Equivalent lumped constants circuit
Schema équivalent à constantes localisées

$$L = \sqrt{2} Z_o / 2 \pi f_o$$

$$C = 1 / 2 \pi f_o \sqrt{2} Z_o$$

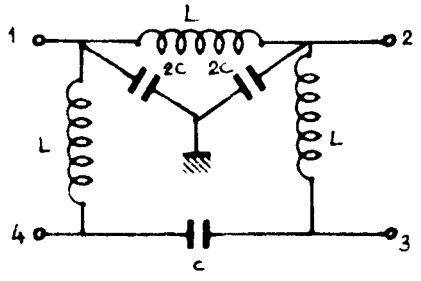

Schéma equivalent modifié pour bande étroite
Equivalent circuit modified for narrow band

Figure III . 3.1

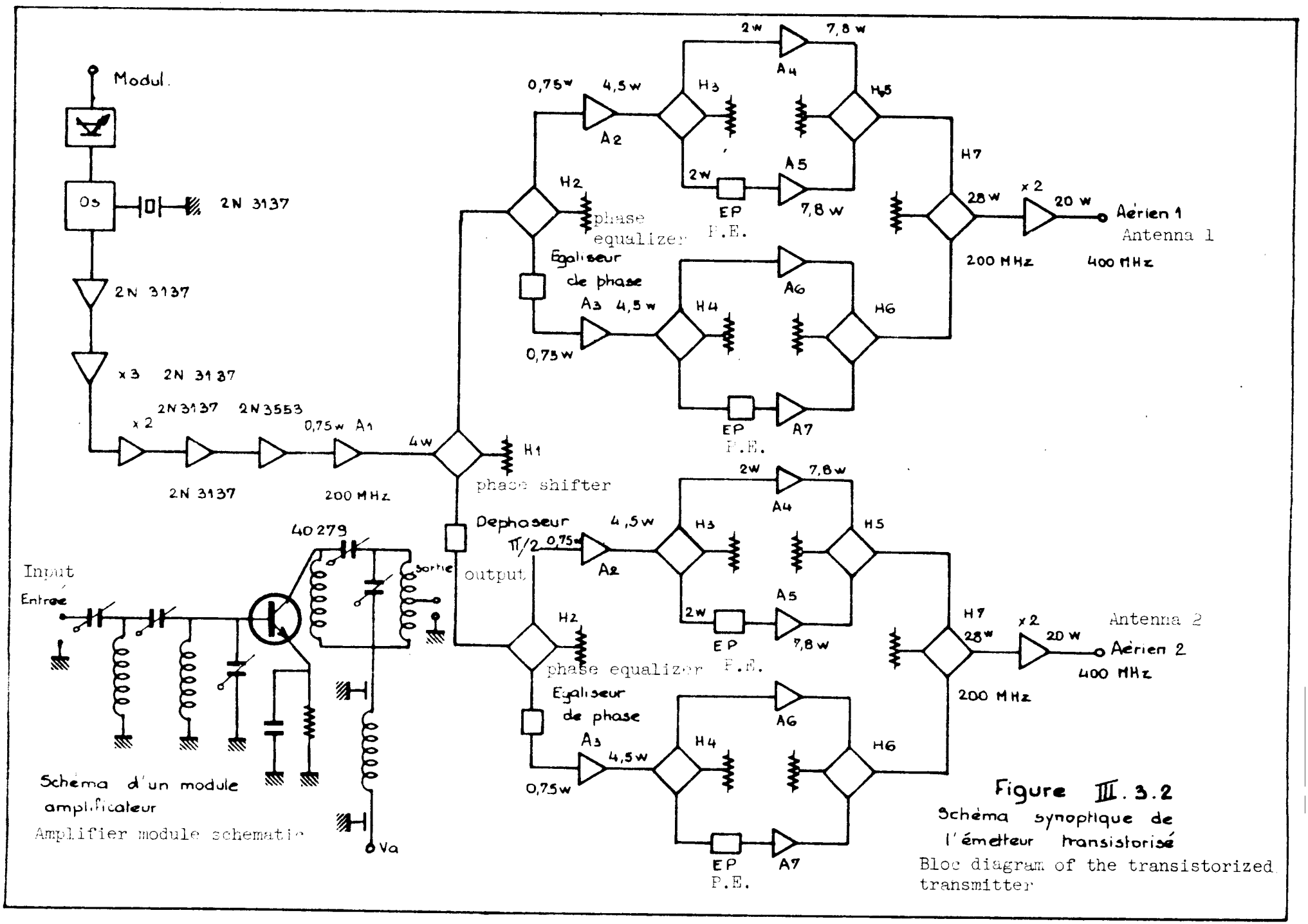

Figure III.3.2

Schéma synoptique de l'émetteur transistorisé

Bloc diagram of the transistorized transmitter

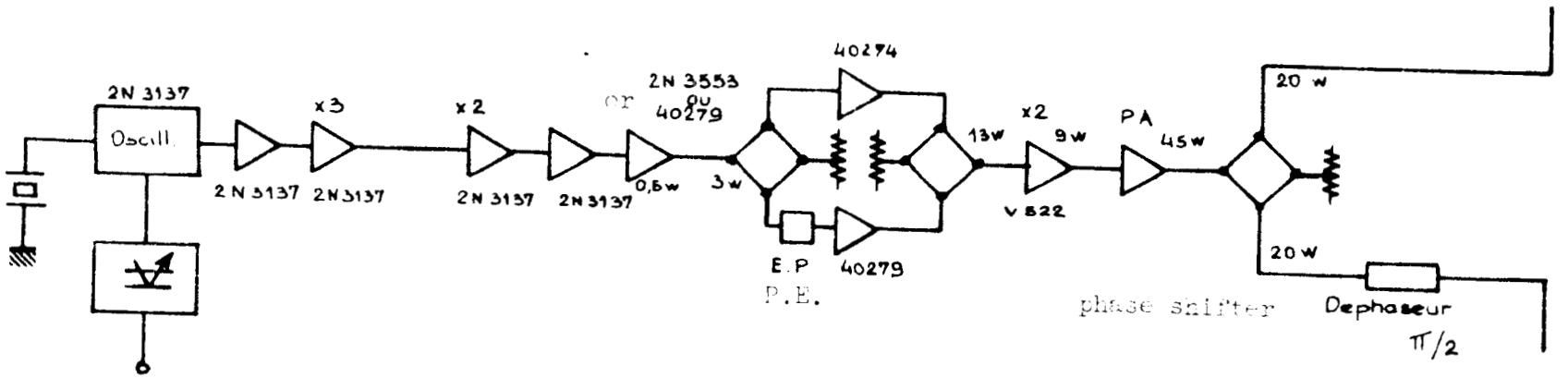

Fig. III. 6.1

Emetteur. PA à tube

Transmitter with tube type P.A.

COMPAGNIE FRANCAISE THOMSON-HOUSTON

GROUPE ÉLECTRONIQUE

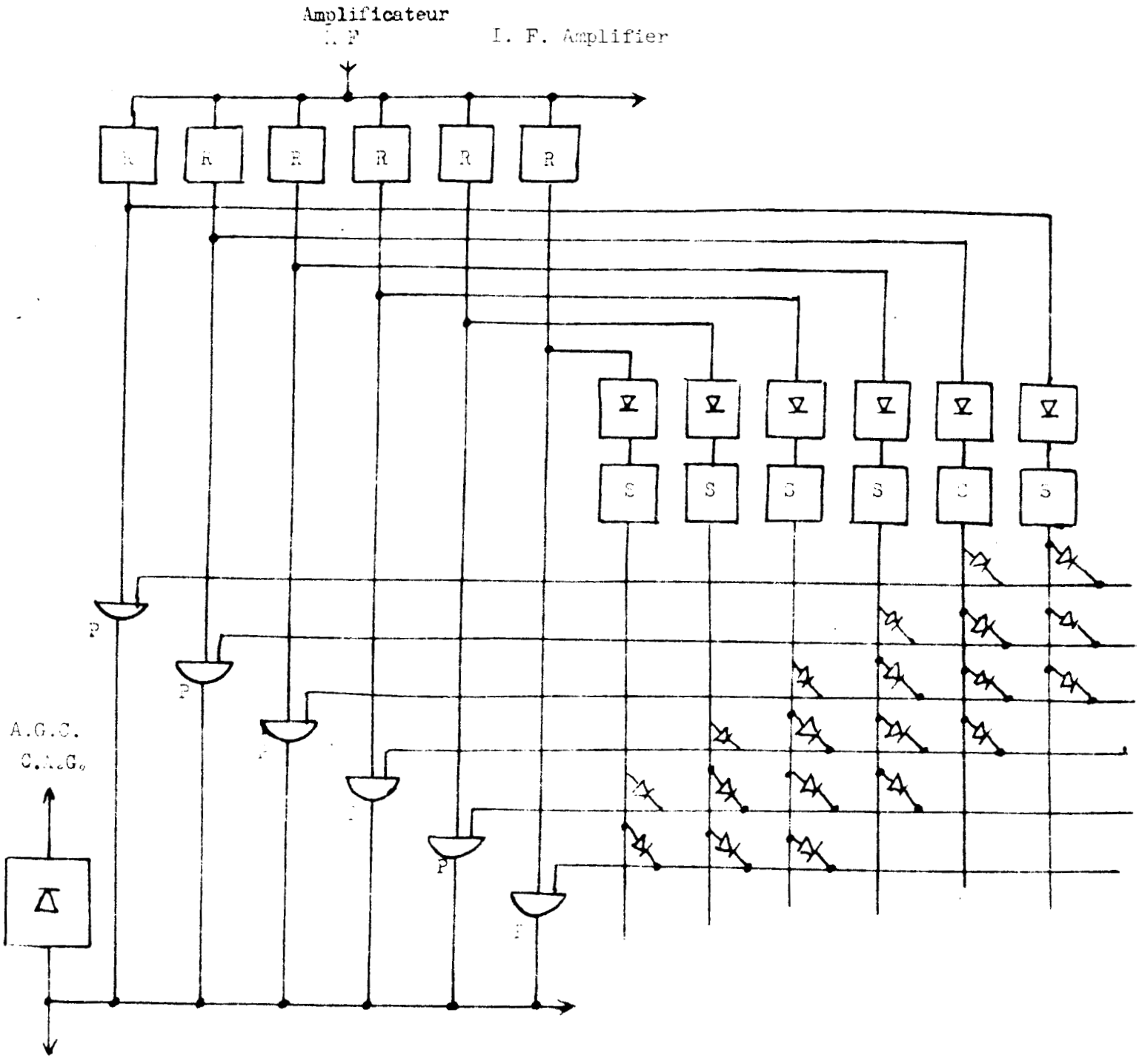

Layout of the narrow band filter system and band selector

Organisation du filtrage à bande étroite et du sélecteur de bande

Figure IV.1c1

RF 597

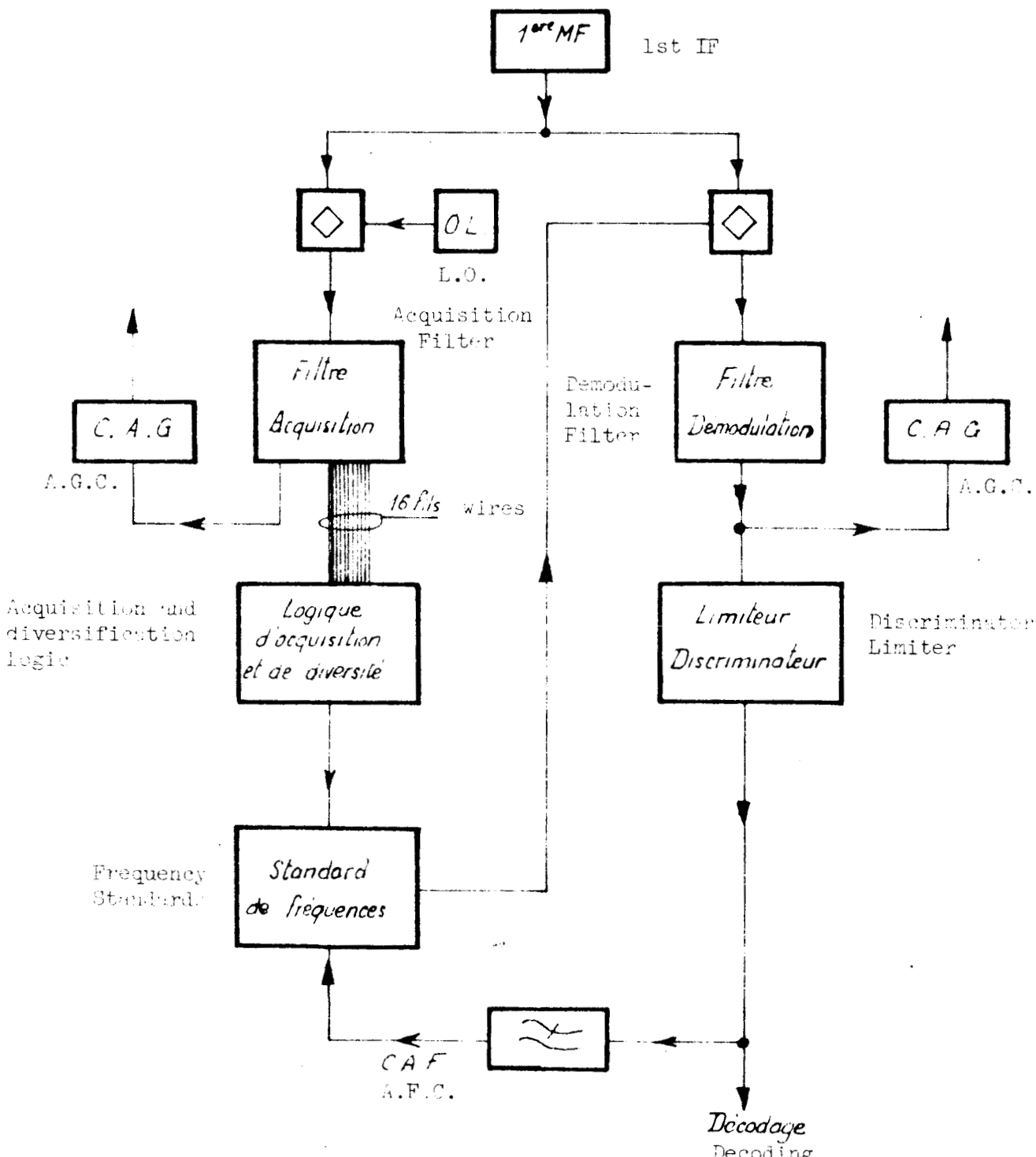
1ère MF
1st IF
OL
L.O.
Acquisition Filter
Filtre Acquisition
Demodulation Filter
Filtre Demodulation
C.A.G
A.G.C.
C.A.G
A.G.C.
16 f/s
wires
Acquisition and diversification logic
Logique d'acquisition et de diversité
Limiteur Discriminateur
Discriminator Limiter
Frequency Standard
Standard de fréquences
CAF
A.F.C.
Décodage
Decoding

Fig. IV.1. 2.

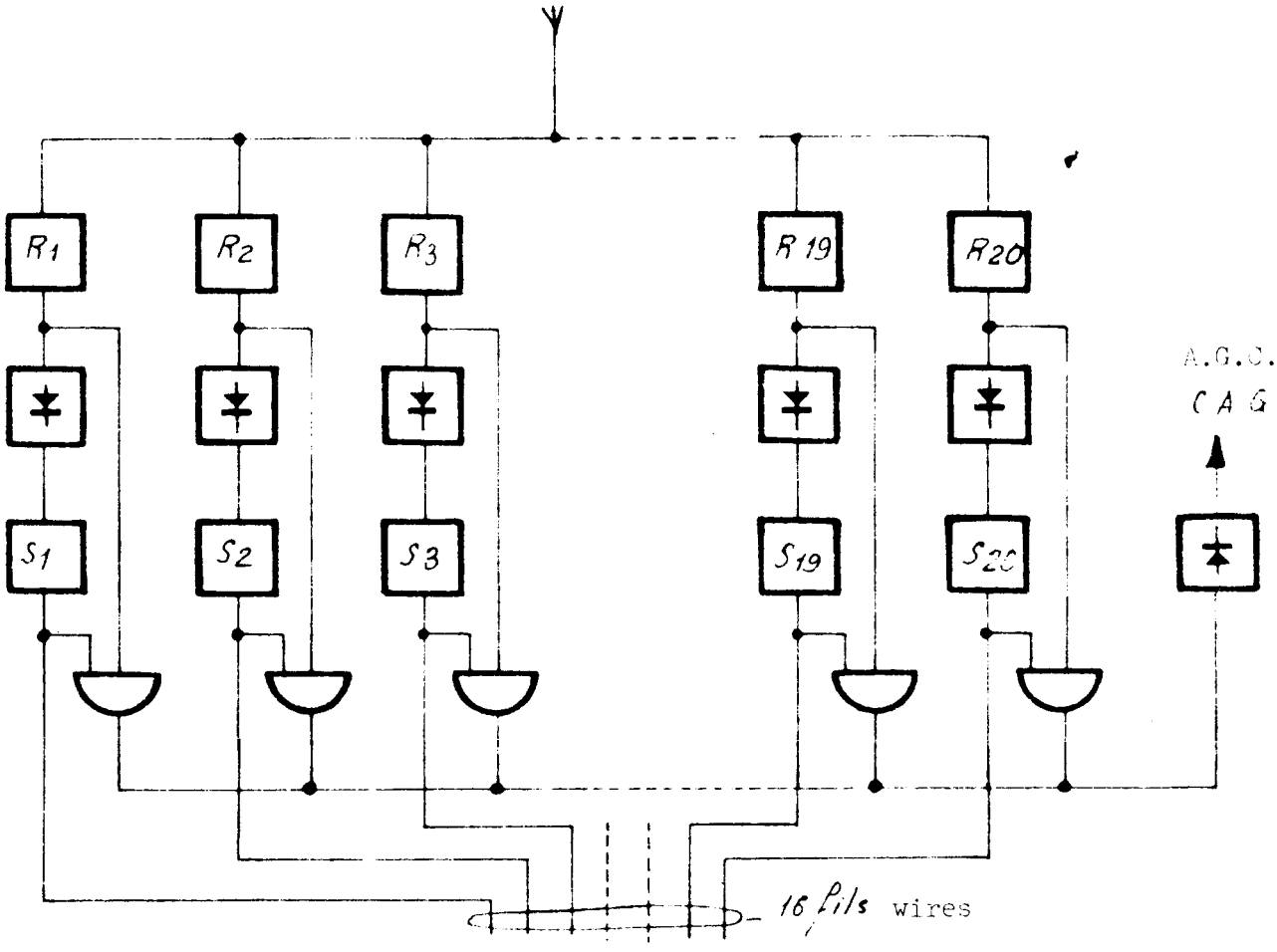

Acquisition Filter

FIG. IV.1.3. FILTRE D'ACQUISITION

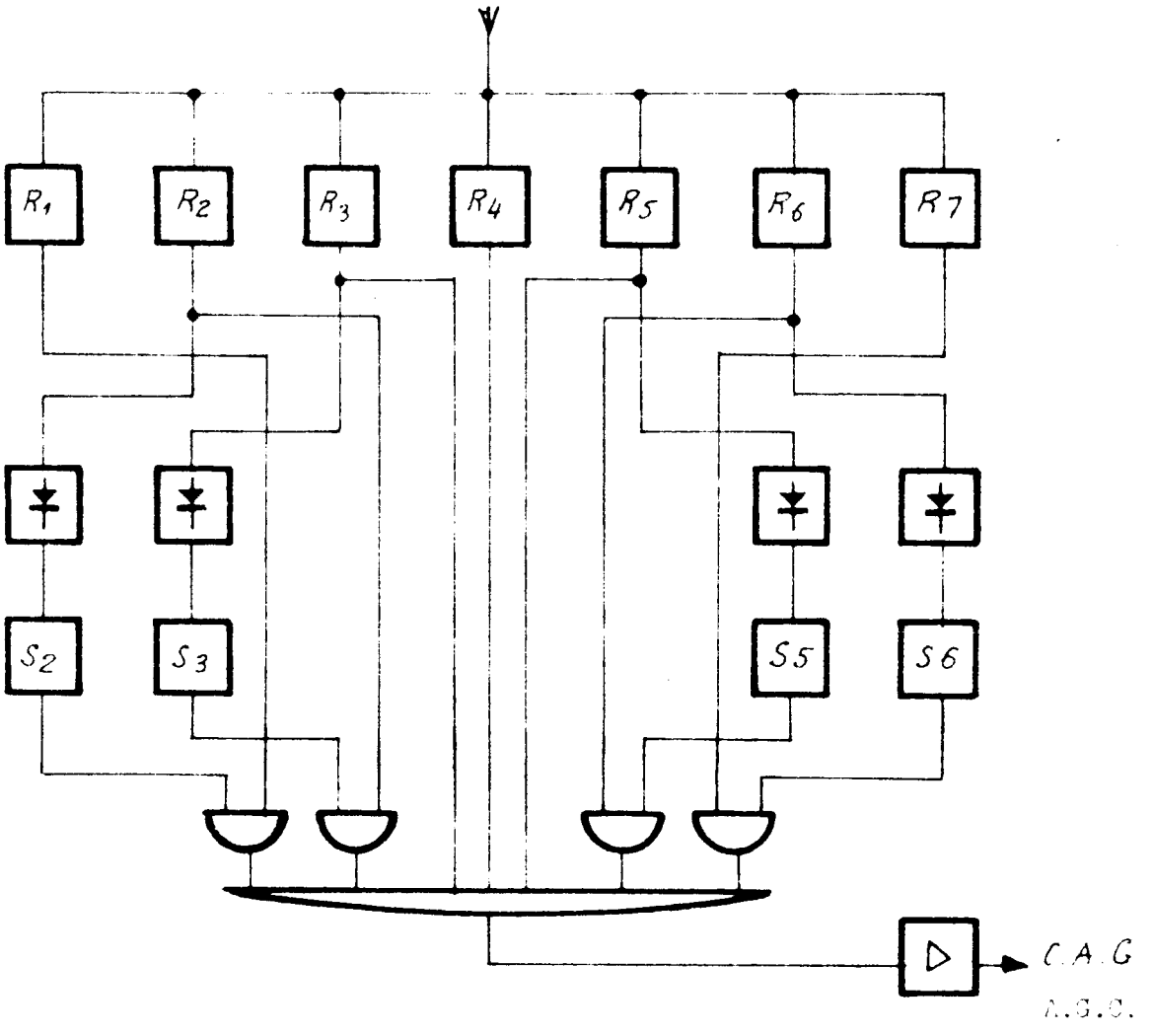

Demodulation Filter

Fig IV.1.4 *FILTRE DE DEMODULATION*

Amplitude and phase curves of a filter made up of 9 poles in parallel

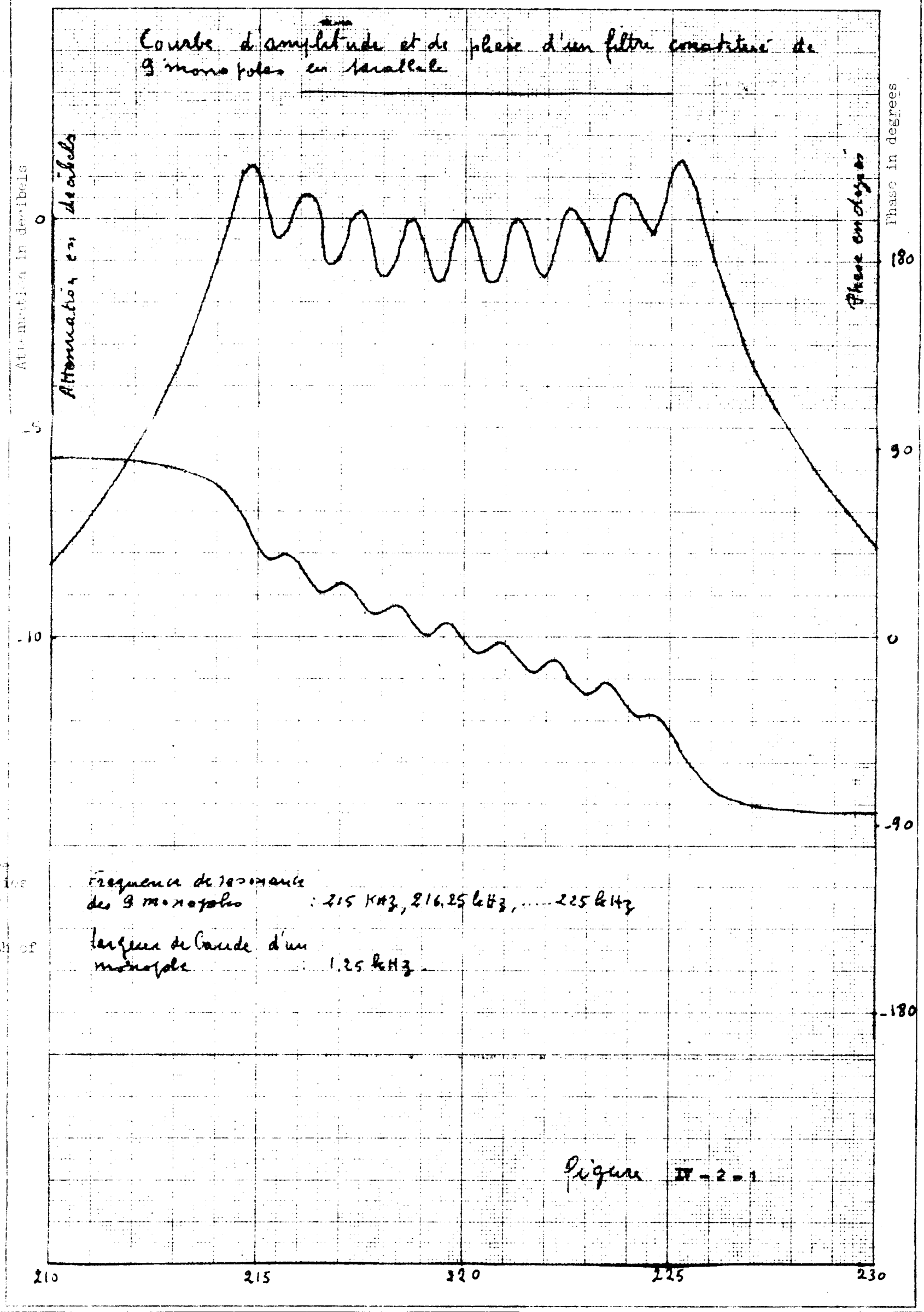

Figure III - 2 - 1

Amplitude and phase curves of a filter made up of 9 poles successively phase shifted at the input by $-\frac{\pi}{2}$.

Courbe d'amplitude et de phase d'un filtre constitué de 9 monopoles déphasés à l'entrée de $-\frac{\pi}{2}$ l'un par rapport à l'autre.

Attenuation in decibels

Attenuation en décibels.

0

-15

-20

Phase en degrés

180

90

0

-90

-180

Resonance frequencies of the 9 poles

Bandwidth of a pole

fréquence de résonance des 9 monopoles : 215 kHz, 216.25 kHz, ... 225 kHz

largeur de bande d'un monopole : 1.25 kHz.

figure IV - 2 - 2

fréquence en kHz

Frequency in kHz

210 215 220 225 230

Amplitude and phase curves of a filter made up of 9 poles successively phase shifted at the input by $-\frac{\pi}{4}$

Courbe d'amplitude et de phase d'un filtre constitué de 9 monopoles déphasés à l'entrée de $-\frac{\pi}{4}$ l'un par rapport à l'autre

Atténuation en db

Attenuation in db

Phase en degrés

Phase in degrees

0

-5

-10

-15

-20

0

-90

-180

-270

-360

Fréquence de resonance des 9 monopoles : 215 KHz, 216.25 KHz, ... 225 kHz

largeur de bande d'un monopole : 2.5 kHz

Resonance frequencies of the 9 poles

Bandwidth of one pole

figure IV - 2 - 4

fréquence en kHz

Frequency in kHz

210 215 220 225 230

Propagation time of a filter made up of 9 poles successively phase shifted at the input by $-\frac{\pi}{2}$.

Temps de propagation d'un filtre constitué de 9 monopoles déphasés à l'entrée de $-\frac{\pi}{2}$ l'un par rapport à l'autre.

Propagation time in µs

Temps de propagation en µsec.

250

200

150

100

50

0

Resonance frequencies of 9 poles

Bandwidth of one pole

fréquence de résonance de 9 monopoles : 215 kHz, 216.25 kHz, ... 225 kHz

largeur de bande d'un monopole : 1.25 kHz

figure IV - 2 - 3

210

215

220

225

230

Frequency in kHz

fréquence en kHz

Propagation time of a filter made up of 9 poles successively phase shifted at the input by $-\frac{\pi}{4}$.

Resonance frequencies of the 9 poles

Bandwidth of one pole

Frequency in kHz

Propagation time in usec

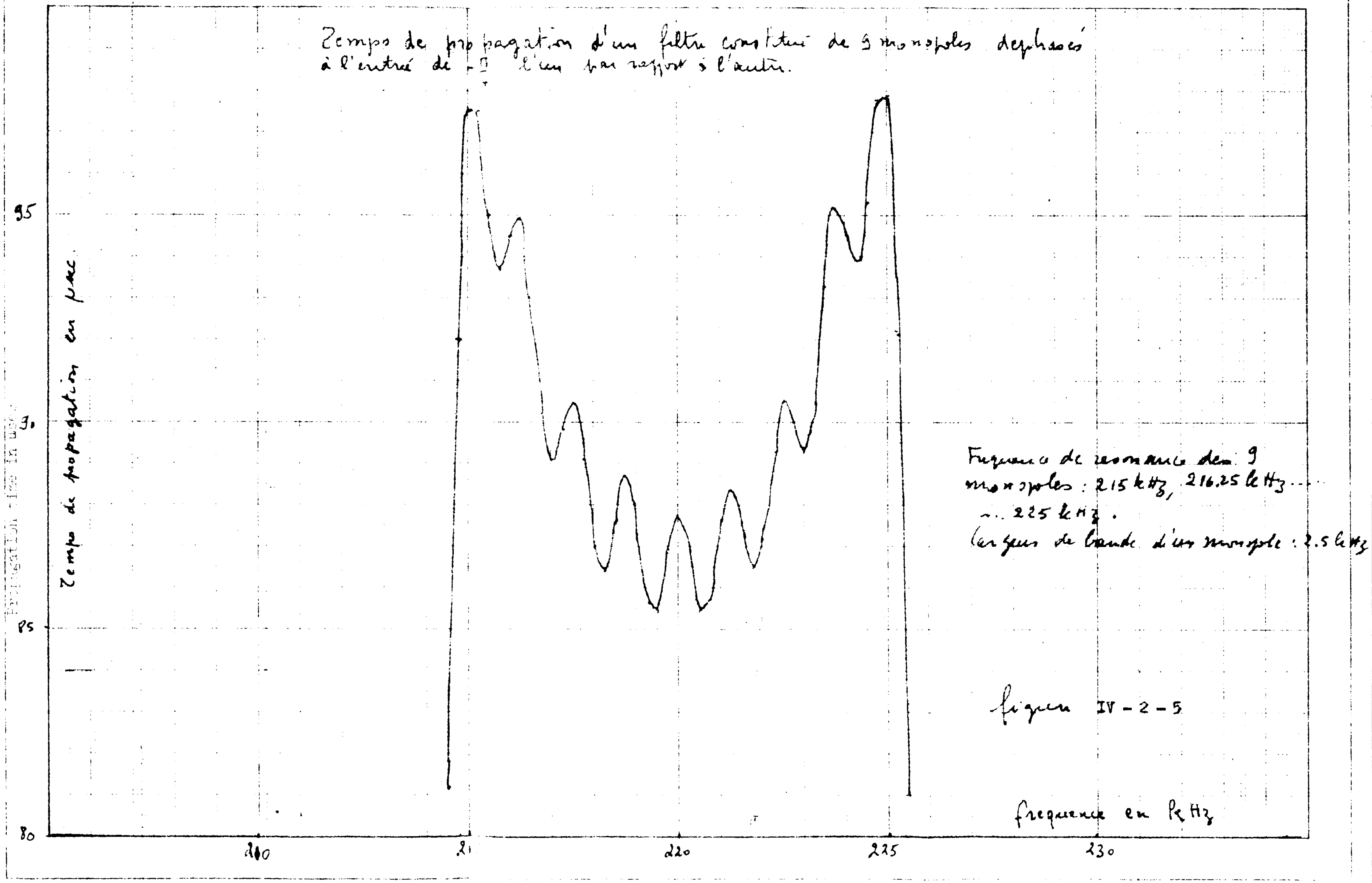

figure IV-2-5

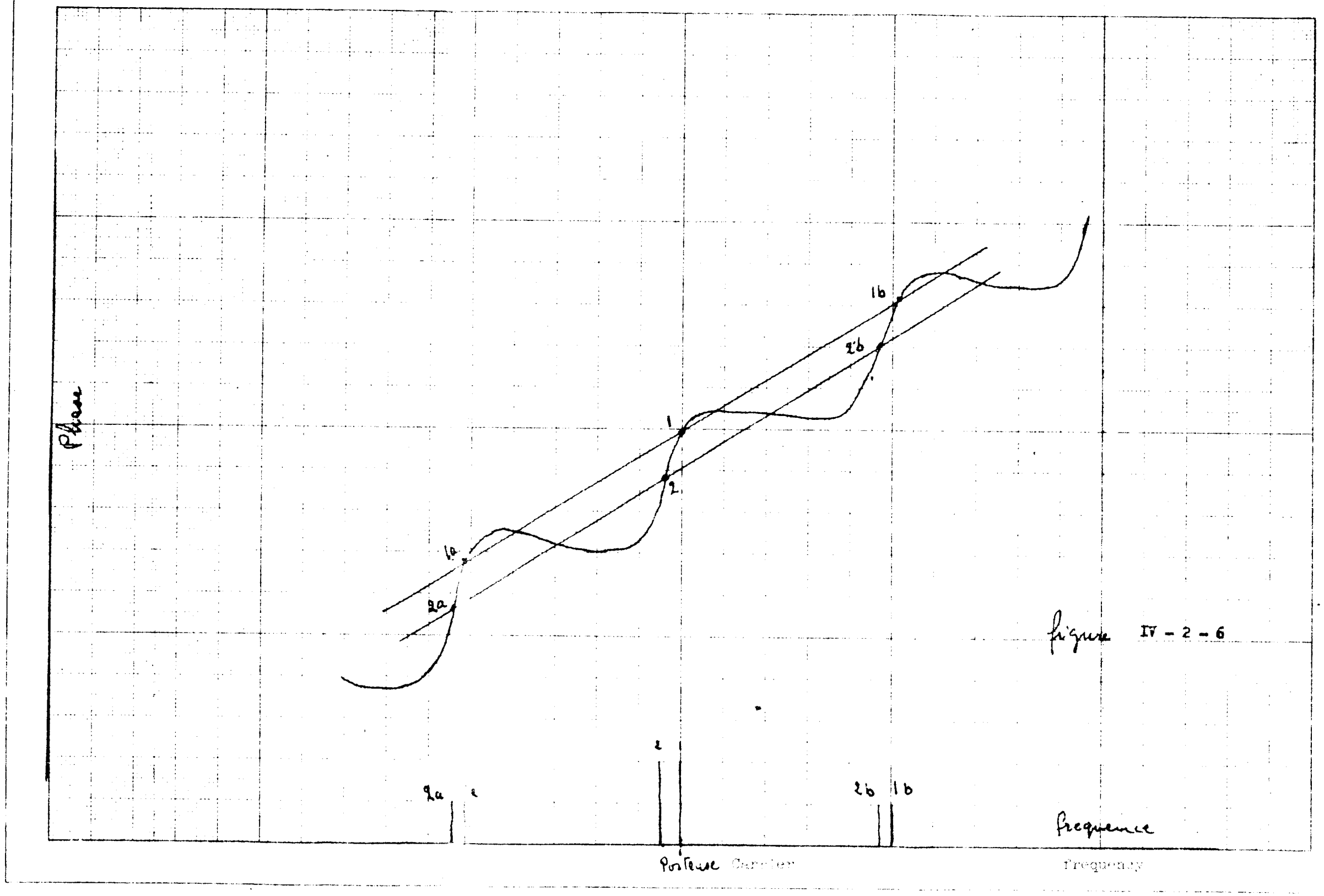
Phase
1b
2b
1
2
1a
2a
2a
c
c
2b
1b
Fréquence
Porteuse Centrale
Frequency

figure IV - 2 - 6

Mean zero deviation vs frequency of a frequency modulated wave going through three, successively phase shifted at the input by - π/2

Déplacement moyen des zéros en fonction de la fréquence d'une onde modulée en fréquence passant dans un filtre constitué de 9 monopôles déphasés à l'entrée de - π/2 l'un par rapport à l'autre.

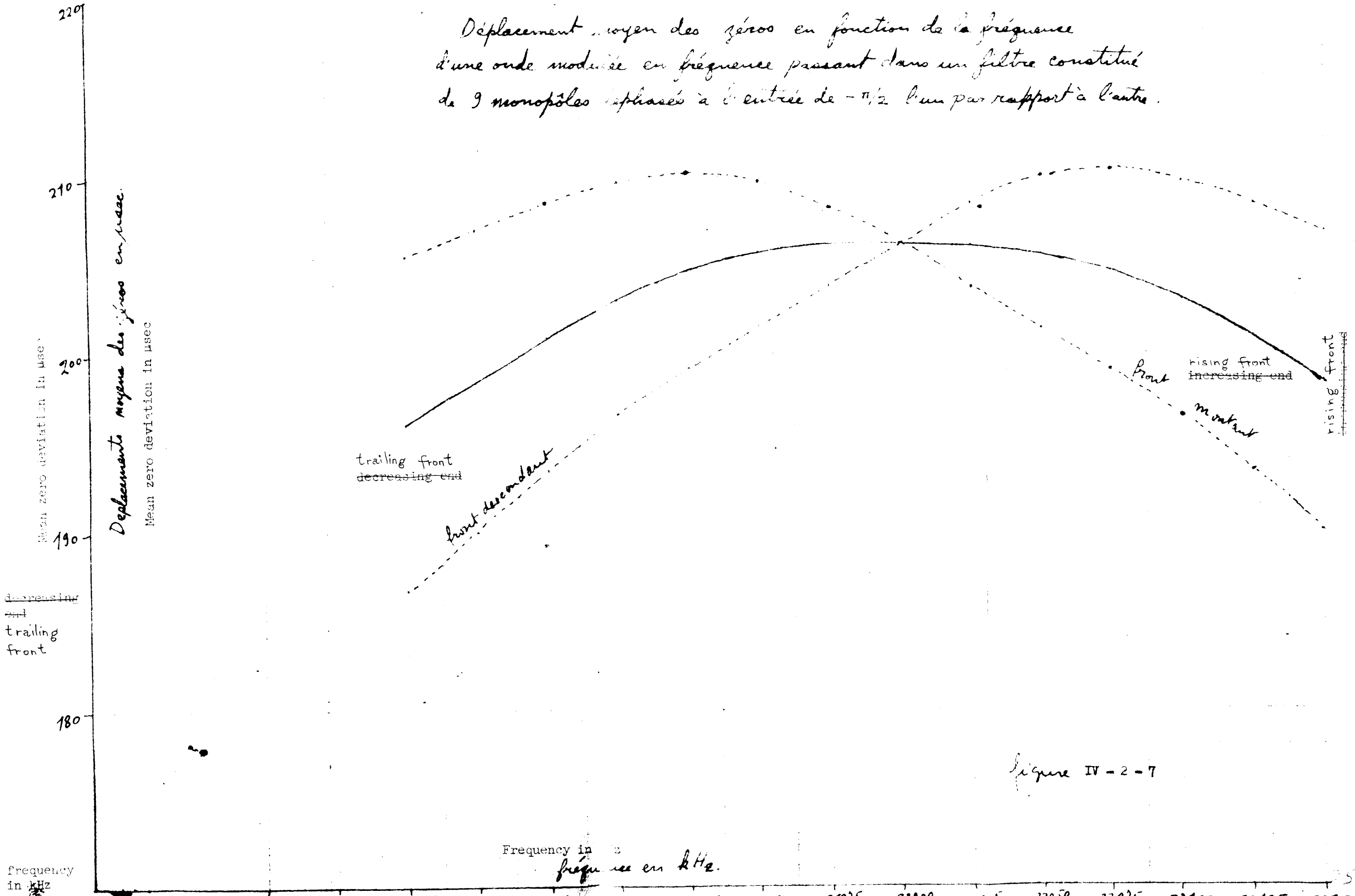

figure IV - 2 - 7

Mean zero deviation vs frequency of a frequency modulated wave going through a filter made up of 9 poles successively phase shifted by - π/4

Deplacement moyen des zeros en fonction de la frequence d'une onde modulée en frequence passant dans un filtre constitué de 9 monopoles dephasés à l'entrée de $-\frac{\pi}{4}$ l'un par rapport à l'autre.

Mean zero deviation in μsec

Deplacement moyen des 9 zeros en μsec.

90

89

88

87

~~Increasing end~~
trailing front

front decroissant

rising front
~~Increasing end~~
front montant

figure IV - 2 - 8

Frequency in kHz
frequence en kHz

217.5 218 218.25 218.5 218.75 219 219.25 219.5 219.75 220 220.25 220.5 220.75 221 221.25

Bandpass filter

FILTRE DE BANDE

COURBE RETARD / FRÉQUENCE

Time Lag vs Frequency Curve

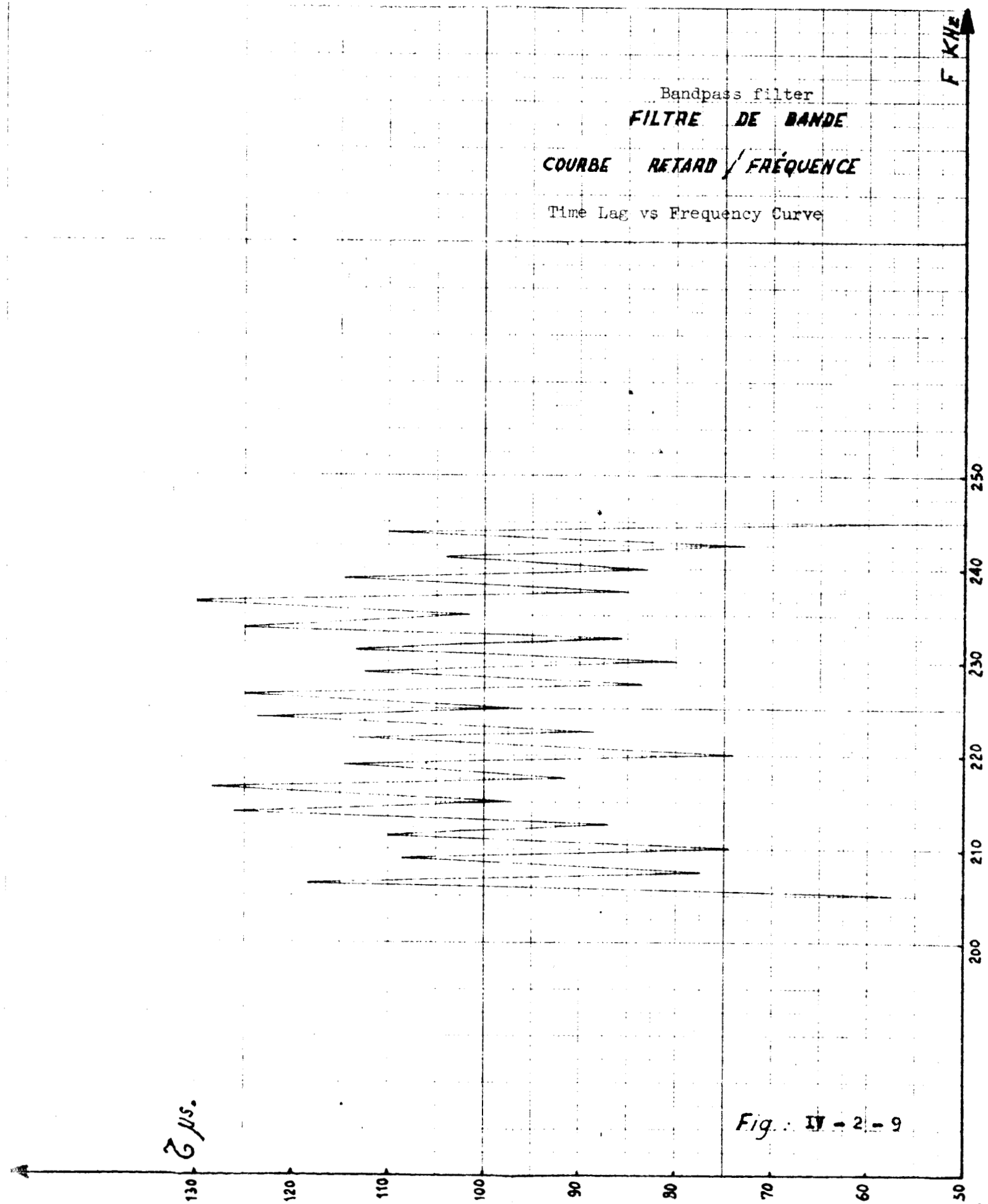

Fig. : IV - 2 - 9

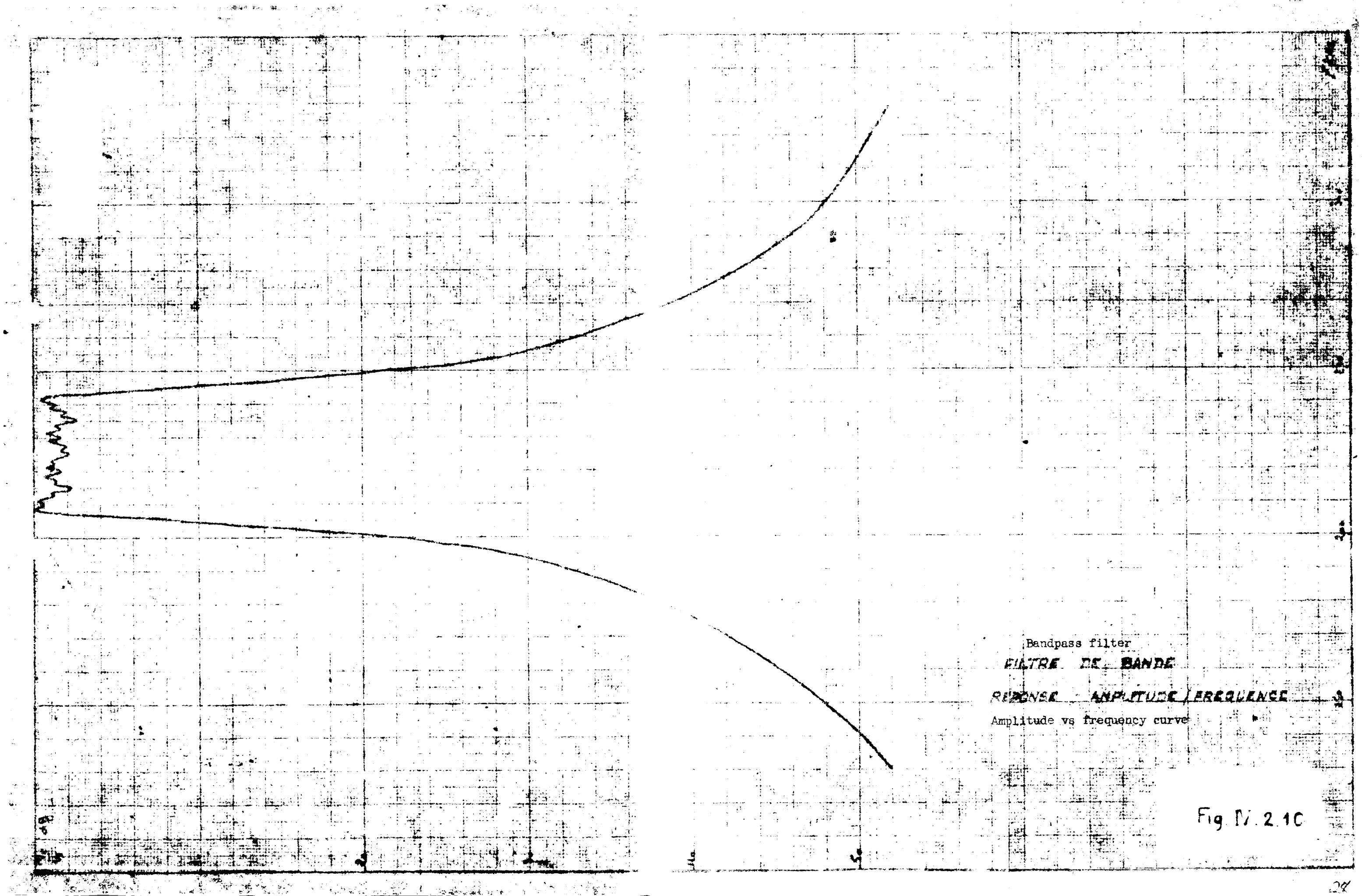

Bandpass filter

FILTRE DE BANDE

RÉPONSE AMPLITUDE / FRÉQUENCE

Amplitude vs frequency curve

Fig. N. 2.10

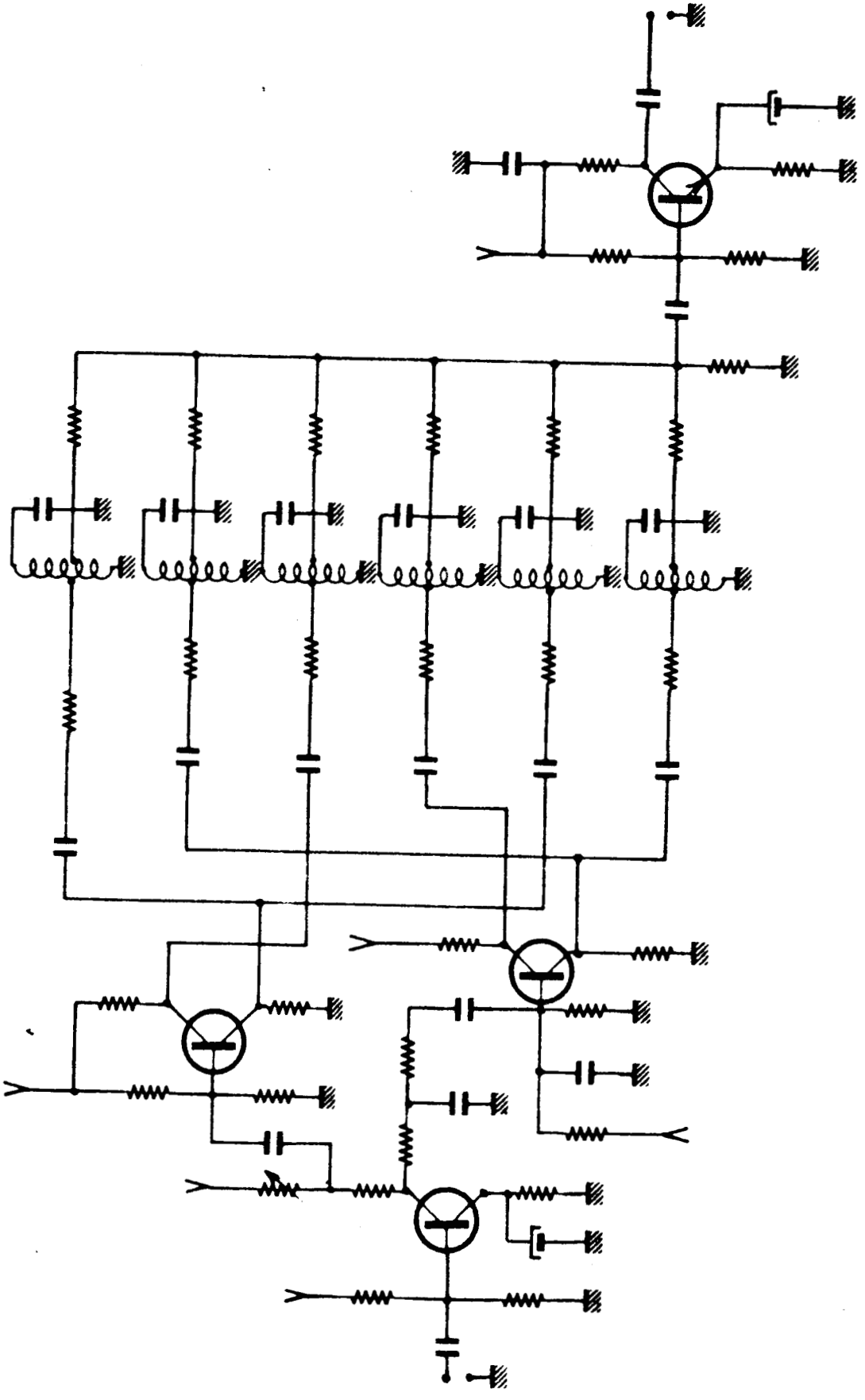

Figure IV. 3.1

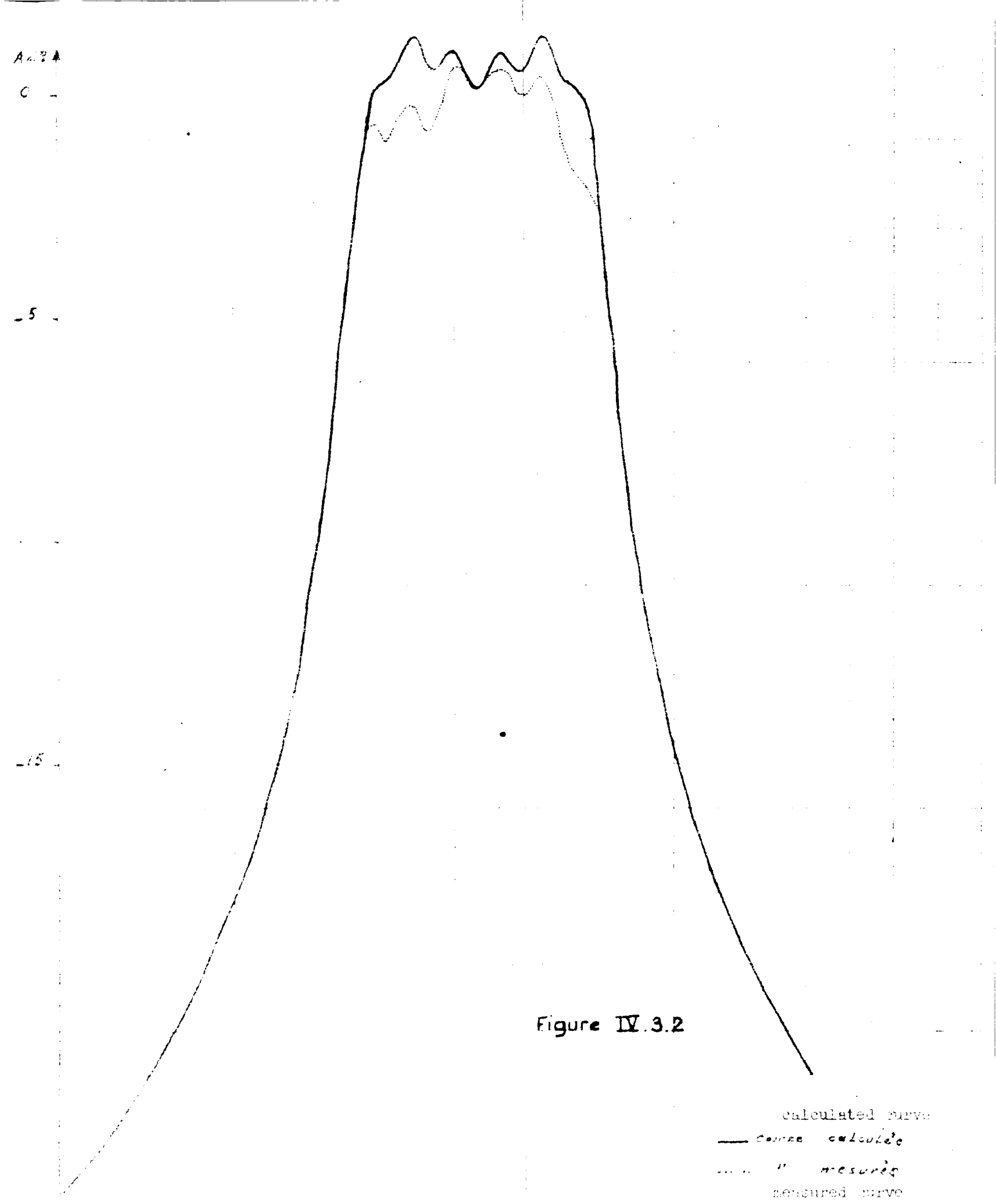
A
0
-5
-15
calculated curve
—— courbe calculée
..... " mesurée
measured curve

Figure IV.3.2

Retard
NS

Lag µsec

rising front
~~increasing end~~
FRONT MONTANT

MOYENNE
average

FRONT DESCENDANT
~~decreasing end~~
trailing front

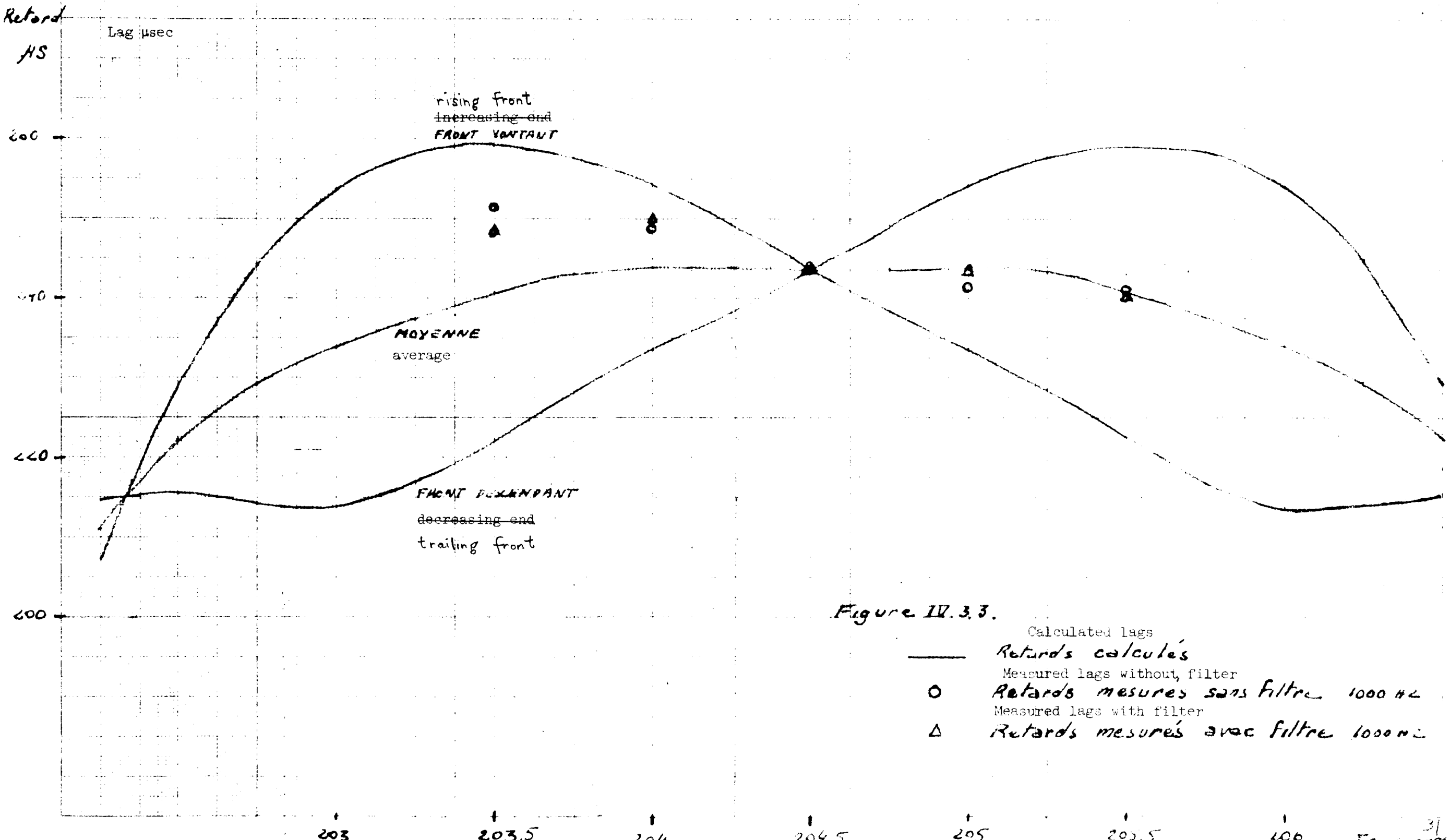

Figure IV.3.3.

Calculated lags
——— Retards calculés
Measured lags without filter
○ Retards mesures sans filtre 1000 Hz
Measured lags with filter
△ Retards mesurés avec filtre 1000 Hz

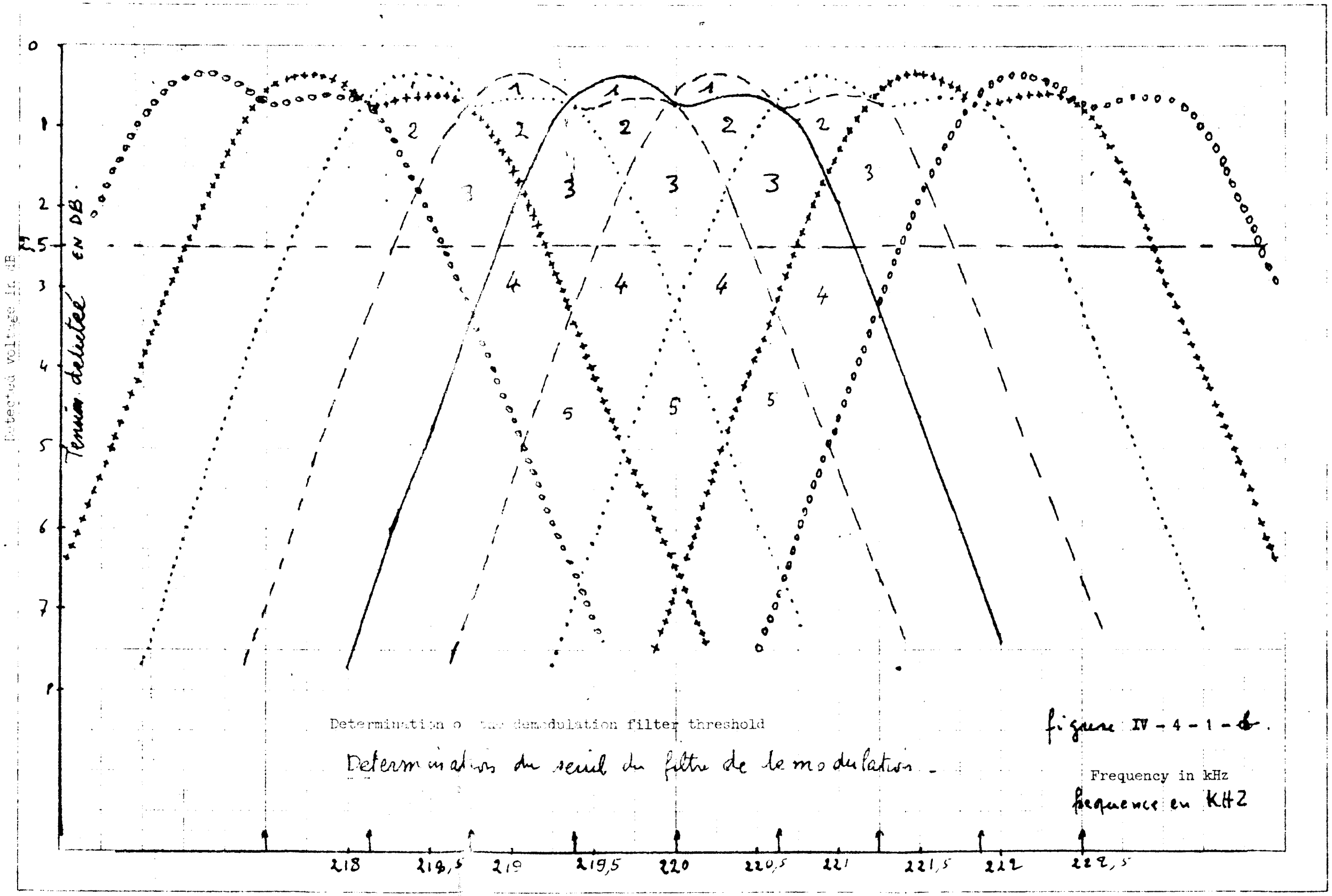

Determination of the demodulation filter threshold

Détermination du seuil du filtre de demodulation.

figure IV - 4 - 1 - b.

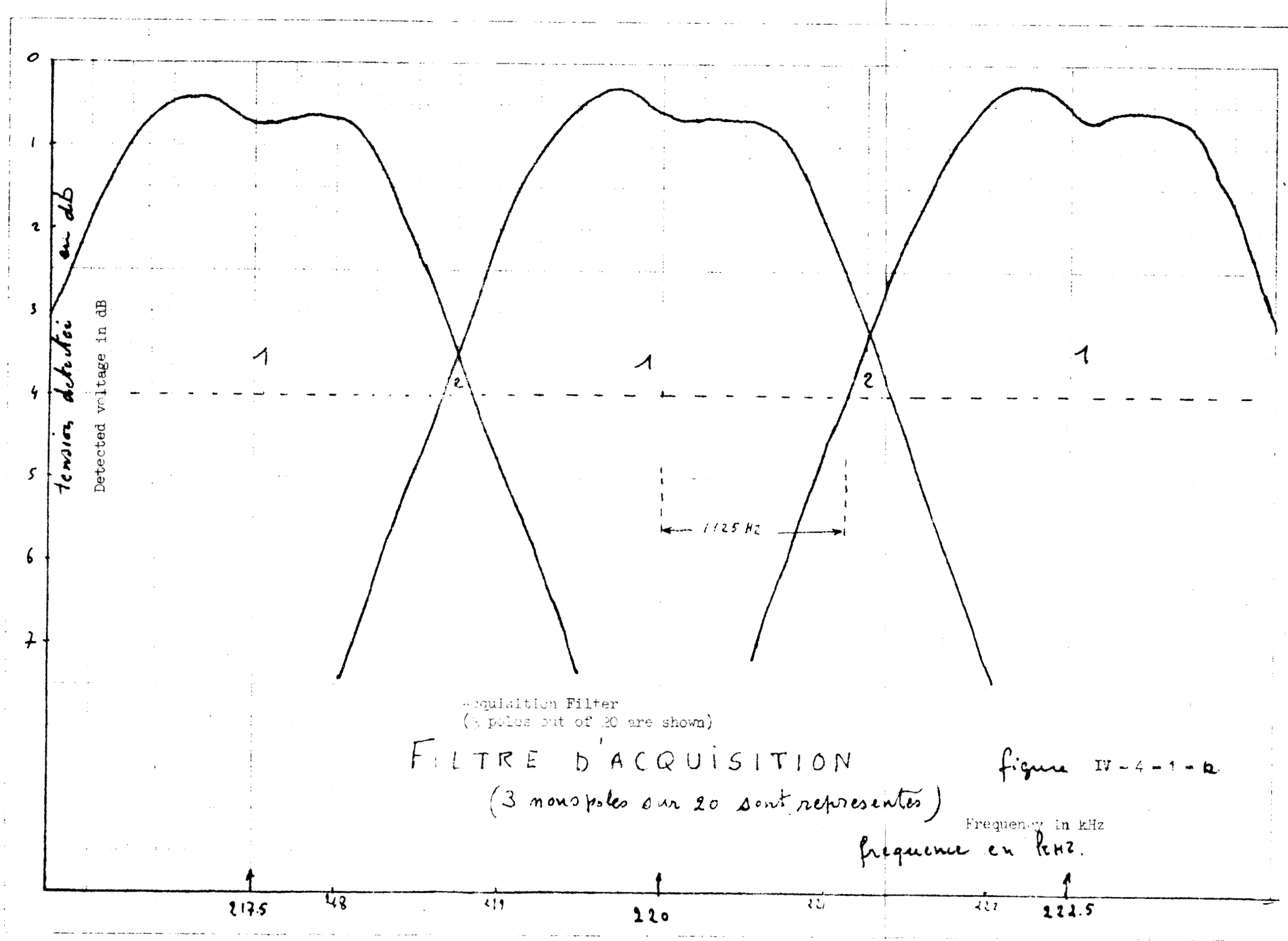

FILTRE D'ACQUISITION (3 monopoles sur 20 sont représentés)

figure IV-4-1-b

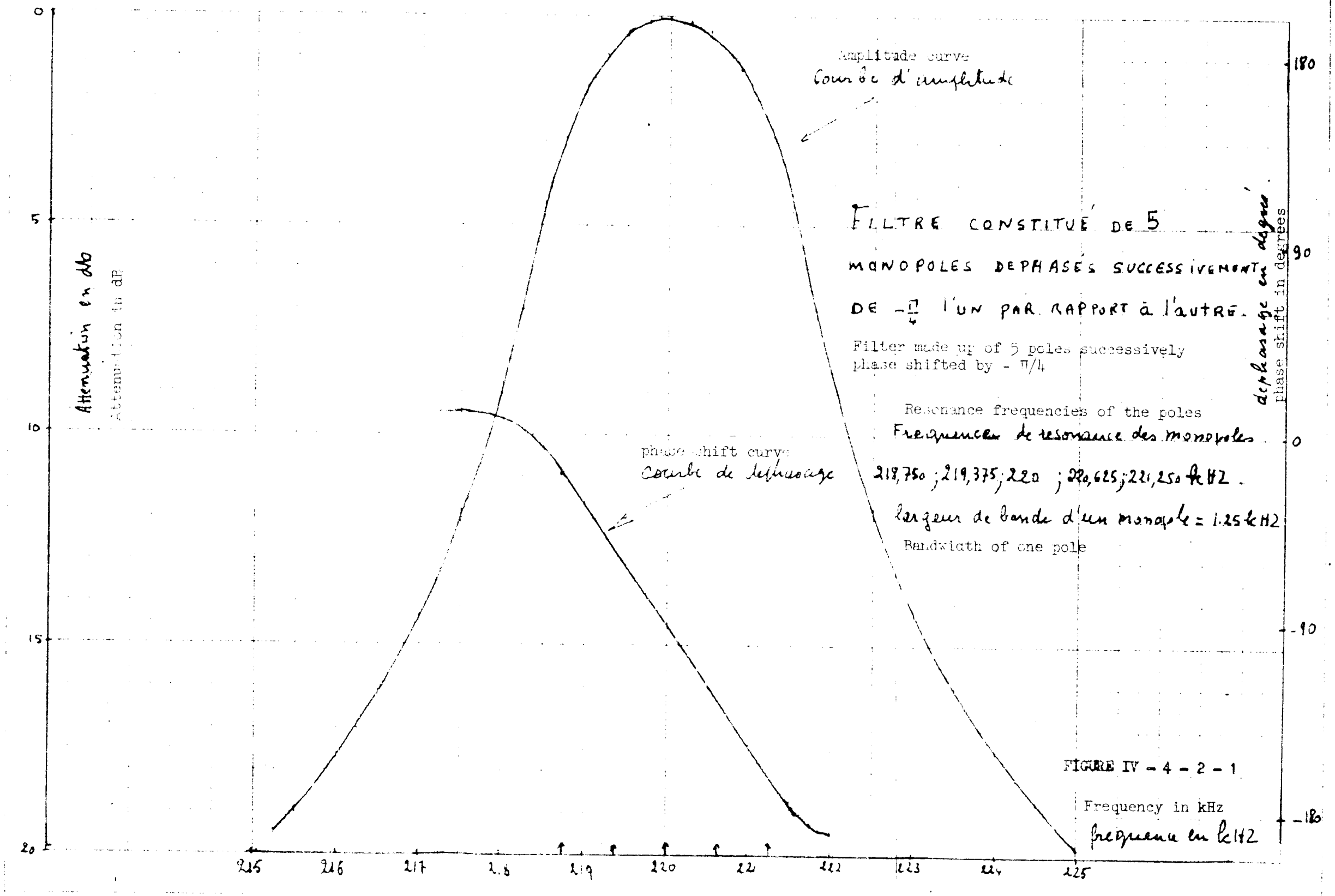

FIGURE IV - 4 - 2 - 1

Zero deviation in usec vs frequency of a frequency modulated wave going through a filter made up of 5 poles, phase shifted at the input by - Π/4.

Déplacement du zero en usec en fonction de la frequence d'une onde modulée en frequence passant dans un filtre constitué de 5 monopôles déphasés à l'entrée de $-\frac{\Pi}{4}$.

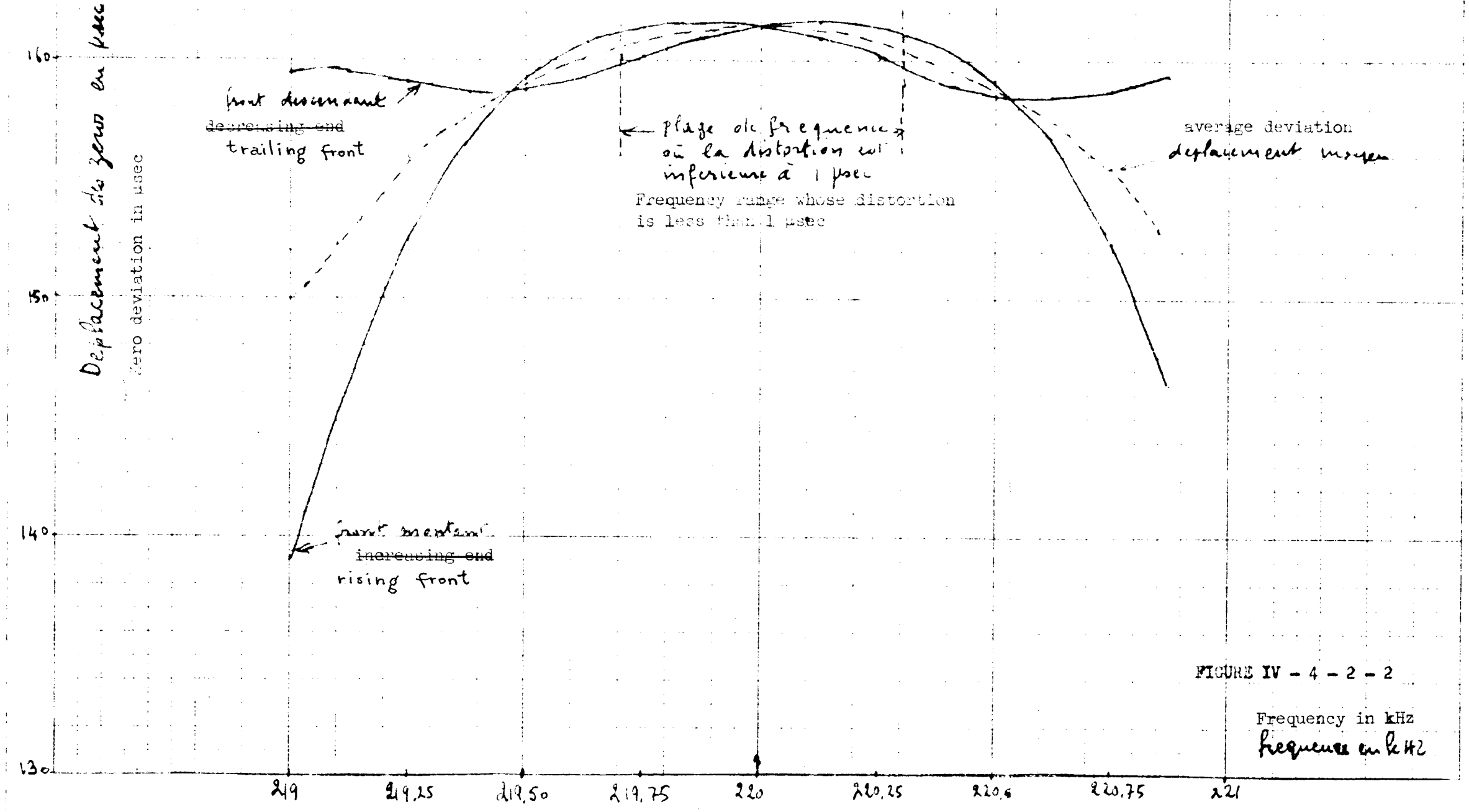

FIGURE IV - 4 - 2 - 2

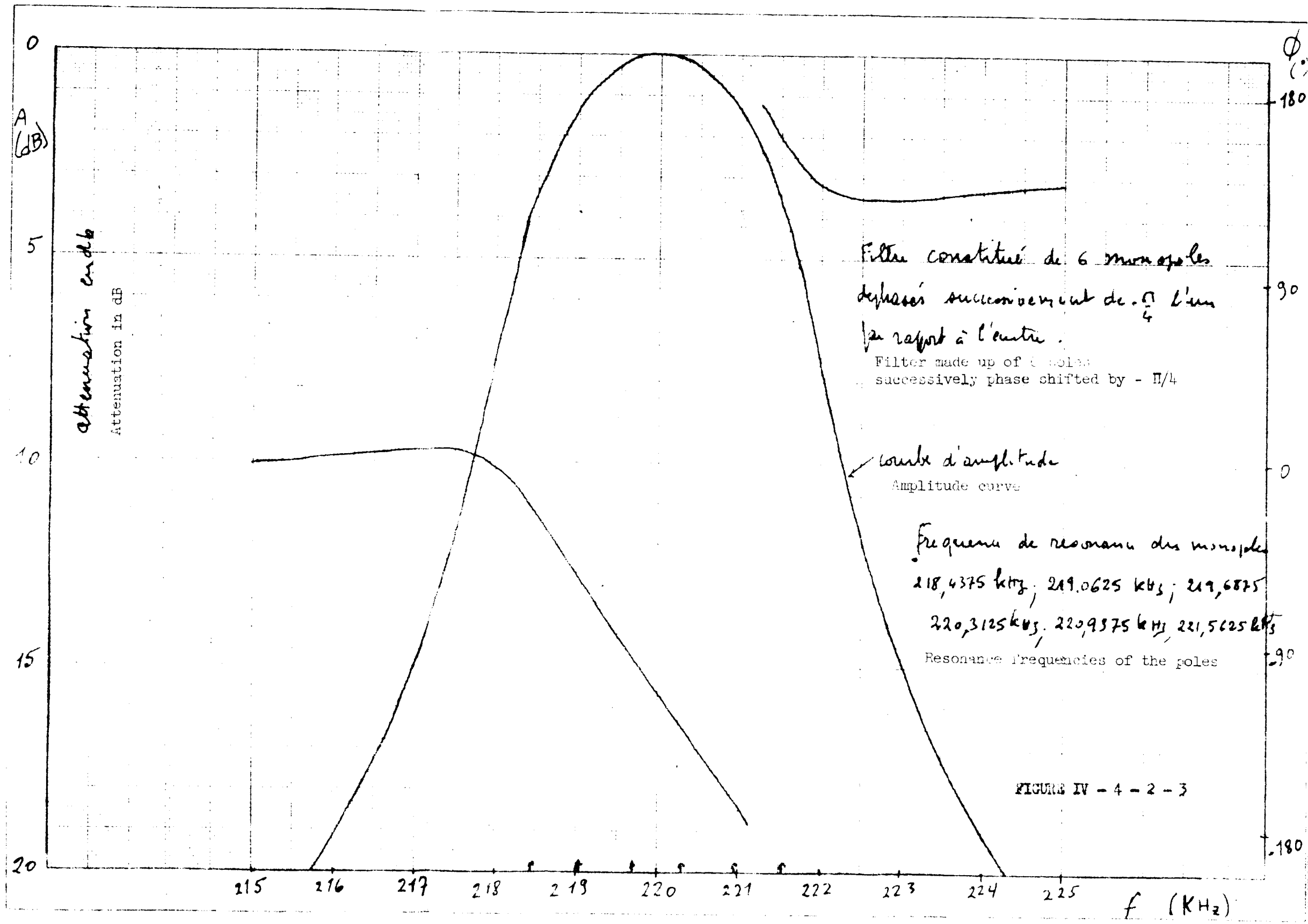

FIGURE IV - 4 - 2 - 3

Zero deviation in µsec vs frequency of a frequency modulated wave going through a filter made up of 6 poles phase shifted by - Π/4

Déplacement des zeros en fonction de la fréquence d'une onde modulée en fréquence passant dans un filtre constitué de 6 monopoles déphasés de -Π/4

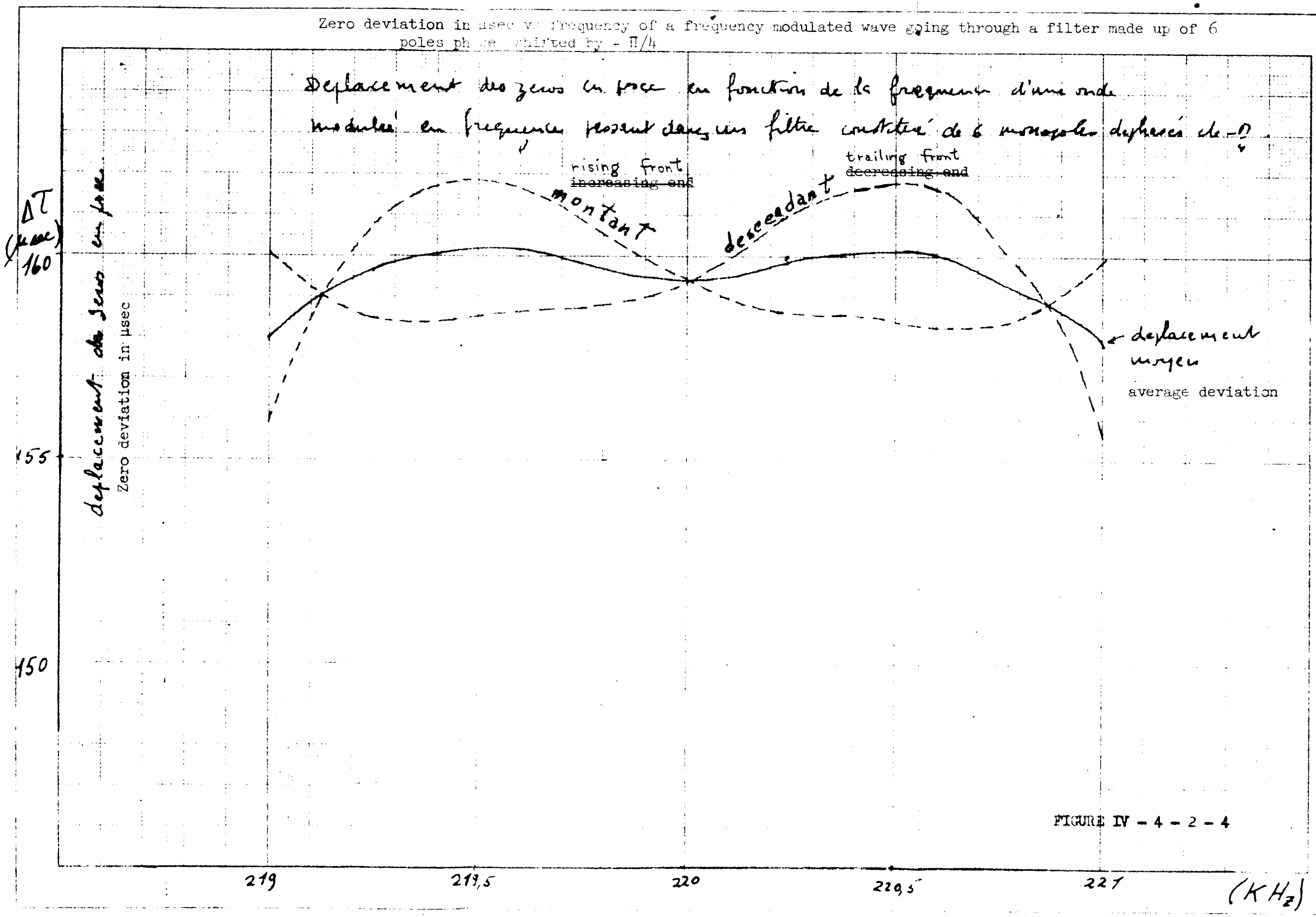

FIGURE IV - 4 - 2 - 4